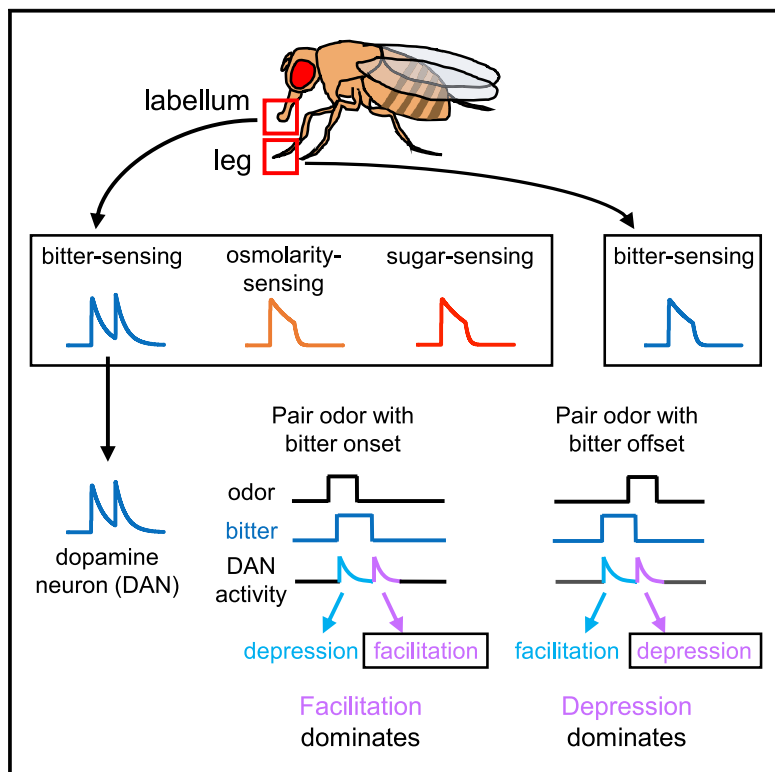


Individual bitter-sensing neurons in *Drosophila* exhibit both ON and OFF responses that influence synaptic plasticity

Graphical abstract



Authors

Anita V. Devineni, Julia U. Deere,
Bei Sun, Richard Axel

Correspondence

anita.devineni@emory.edu (A.V.D.),
ra27@columbia.edu (R.A.)

In brief

Devineni et al. show that individual bitter-sensing neurons of the fly labellum are activated at both the onset and removal of bitter, in contrast to other types of taste neurons. These response dynamics are transmitted to downstream dopaminergic neurons, and the strong response to bitter removal impacts synaptic plasticity during learning.

Highlights

- Taste sensory neurons in *Drosophila* show varying response dynamics
- Individual bitter-sensing neurons of the labellum display strong ON and OFF responses
- OFF responses are generated cell-intrinsically through canonical bitter receptors
- Bitter OFF responses in dopaminergic neurons influence synaptic plasticity



Article

Individual bitter-sensing neurons in *Drosophila* exhibit both ON and OFF responses that influence synaptic plasticity

Anita V. Devineni,^{1,3,6,*} Julia U. Deere,^{1,4} Bei Sun,^{1,5} and Richard Axel^{1,2,*}

¹Zuckerman Mind Brain Behavior Institute, Columbia University, 3227 Broadway, New York, NY 10027, USA

²Howard Hughes Medical Institute, Columbia University, New York, NY 10032, USA

³Present address: Department of Biology, Emory University, Atlanta, GA 30322, USA

⁴Present address: Rockefeller University, New York, NY 10065, USA

⁵Present address: Sackler School of Medicine, New York State/American Program of Tel Aviv University, Tel Aviv, Israel

⁶Lead contact

*Correspondence: anita.deveneni@emory.edu (A.V.D.), ra27@columbia.edu (R.A.)

<https://doi.org/10.1016/j.cub.2021.10.020>

SUMMARY

The brain generates internal representations that translate sensory stimuli into appropriate behavior. In the taste system, different tastes activate distinct populations of sensory neurons. We investigated the temporal properties of taste responses in *Drosophila* and discovered that different types of taste sensory neurons show striking differences in their response dynamics. Strong responses to stimulus onset (ON responses) and offset (OFF responses) were observed in bitter-sensing neurons in the labellum, whereas bitter neurons in the leg and other classes of labellar taste neurons showed only an ON response. Individual labellar bitter neurons generate both ON and OFF responses through a cell-intrinsic mechanism that requires canonical bitter receptors. A single receptor complex likely generates both ON and OFF responses to a given bitter ligand. These ON and OFF responses in the periphery are propagated to dopaminergic neurons that mediate aversive learning, and the presence of the OFF response impacts synaptic plasticity when bitter is used as a reinforcement cue. These studies reveal previously unknown features of taste responses that impact neural circuit function and may be important for behavior. Moreover, these studies show that OFF responses can dramatically influence timing-based synaptic plasticity, which is thought to underlie associative learning.

INTRODUCTION

Organisms have evolved diverse mechanisms to recognize sensory stimuli in the environment and transmit this information to the brain. The efficient translation of external stimuli into behavior engages sensory neurons that may respond to the same stimulus in different ways. For example, ON cells respond to the onset of a stimulus or an increase in its intensity, whereas OFF cells respond to stimulus offset or decreased intensity. In most sensory systems, ON cells predominate, but OFF responses have been observed in visual,¹ auditory,² somatosensory,³ and chemosensory^{4,5} pathways. ON-OFF cells that respond to both stimulus onset and offset are also observed.^{6–9} The disappearance of a stimulus may be as relevant to an organism as its appearance. An OFF response enables the nervous system to detect stimulus decrements more rapidly and reliably than the decay of the ON response. Computational modeling suggests that ON-OFF systems provide more efficient information coding in noisy conditions.¹⁰ Thus, OFF responses have been proposed to underlie the perception of stimulus duration, disappearance, and gaps in a stream of stimuli.^{2,11–13}

OFF responses may also elicit behaviors distinct from ON responses. For example, the onset of an attractive odor causes

an animal to orient upwind or move forward, whereas odor offset induces local search behaviors, such as turning.^{14–16} In *C. elegans*, these distinct behaviors are mediated by the AWA and AWC neurons, which respectively respond to odor onset or offset.^{17,18} The onset and offset of a stimulus may also reinforce opposing behaviors during learning. A prominent example is “relief learning,” in which cues associated with the end of a punishment become attractive, whereas cues associated with punishment onset become aversive.^{19–21} The ability of ON and OFF responses to elicit or reinforce different behaviors is most easily accomplished if these responses occur in different populations of cells.^{1,17,18,22} However, individual cells can exhibit both ON and OFF responses,^{2,7} and more complex processing is required to interpret these two responses differently and elicit different behaviors.

In the taste system, different taste modalities are typically encoded by distinct populations of sensory cells that drive innate behavioral responses.²³ Sugar-sensing cells promote feeding, whereas bitter-sensing cells elicit aversion and suppress feeding. Insects possess taste sensory neurons in multiple organs, including the legs, wings, and labellum (the distal segment of the proboscis).²⁴ These external taste neurons enable insects to rapidly sample different substrates as they navigate an



environment, and insects use taste cues to guide ongoing behaviors, including feeding, locomotion,^{25,26} egg-laying,²⁷ grooming,²⁸ and courtship.^{29,30} In this study, we investigate the timing of gustatory responses in *Drosophila* and observe that different taste sensory neurons show striking differences in their response dynamics. Individual bitter-sensing neurons of the labellum show both ON and OFF responses, whereas bitter neurons of the leg exhibit only an ON response. These response dynamics are propagated to downstream dopaminergic neurons and influence synaptic plasticity during learning.

RESULTS

Taste neurons vary in the temporal properties of their responses

We analyzed the timing of *Drosophila* taste responses by performing calcium imaging at the axon terminals of sensory neurons within the subesophageal zone (SEZ) of the brain (Figure 1A). Small drops of tastants were delivered to the labellum or foreleg. Labellar bitter-sensing neurons responded strongly to bitter stimuli such as quinine, denatonium, and lobeline (Figures 1A–1C). These bitter neurons showed peaks in activity when the stimulus was presented (ON response) and removed (OFF response). The magnitude of the OFF response was often similar or larger than that of the ON response, and both responses were closely time-locked to the stimulus (Figures 1B and 1C). The ON response exhibited marked adaptation: the response decayed rapidly during the stimulus presentation (Figure 1C). In contrast to bitter-sensing neurons, labellar sugar-sensing neurons displayed a strong ON response but no OFF response when stimulated with sucrose (Figures 1D and 1G). We also imaged the osmolarity-sensing neurons, which respond to water as well as other low osmolarity solutions,³¹ including the same bitter solutions used to activate bitter-sensing neurons. These neurons showed strong ON responses but no OFF responses (Figures 1D and 1G). Thus, the OFF response is specific to the bitter taste modality.

We then imaged the responses of bitter neurons in the leg (tarsus) and found that they showed strong ON responses, but no OFF response, to all three bitter compounds tested (Figures 1E, 1G, and S1; a single exception is shown in Figures S1B and S1C). Tarsal bitter neurons also showed far less adaptation of the ON response than labellar bitter neurons (Figures 1E, 1F, and S1). These results suggest that bitter neurons in the leg and labellum encode the same taste stimuli in fundamentally different ways: the leg signals the presence or absence of bitter, whereas the labellum signals bitter onset and offset.

Further characterization of the bitter OFF response

Our initial experiments focused on one class of labellar bitter neurons (S-a). Four classes of labellar bitter neurons have been identified based on the bitter receptors they express: S-a, S-b, I-a, and I-b.³² We therefore asked whether all four classes show both ON and OFF responses. We used *Gal4* lines that target each class with either complete (S-a, S-b, and I-b) or partial (I-a) specificity.³² Each class of neurons showed both ON and OFF responses to at least a subset of bitter compounds (Figures 2A–2C). Quinine and denatonium induced the strongest OFF responses, lobeline induced a weaker OFF response, and caffeine

induced little to no OFF response (Figures 2A–2C). There was no correlation between the peak ON and OFF response (Figure 2D).

We recapitulated the stimulus dependence of the OFF response using a *Gal4* line that labels all labellar bitter neurons (*Gr33a-Gal4*; Figures 2E and 2F).³² Interestingly, we also found that L-canavanine induced an ON response but no OFF response at all (Figures 2E and 2F). The observation that a bitter compound can activate bitter-sensing neurons without eliciting an OFF response implies that the OFF response is not a general property of the neurons. Decoding analyses using a linear classifier revealed that the OFF response performed far better in decoding bitter identity than the ON response (Figure S2A). Bitter responses from the leg (Figure 1E) performed poorly in decoding stimulus identity whether we used the ON response, the OFF response (which is close to zero), or both (Figure S2B). Thus, bitter responses in the labellum contain much more information about bitter identity than responses in the leg, and this is largely due to the OFF response.

We next tested whether the OFF response depends on bitter concentration. The lowest bitter concentrations that were tested elicited ON responses but no OFF response (Figures 2G and 2H). As the bitter concentration was increased, the OFF response, as well as the ratio of the OFF to ON response, generally increased in magnitude (Figures 2G and 2H). Decoder analyses revealed that the OFF response performed much better than the ON response in decoding bitter concentration (Figures S2C and S2D). Additional experiments revealed that bitter response dynamics are not modulated by factors such as sex, hunger, or the presence of an appetitive tastant (Figures S2E–S2G). Together, these results show that bitter OFF responses are observed in all classes of labellar bitter neurons, and bitter response dynamics depend on stimulus identity and concentration.

In other systems, such as the visual system, ON and OFF responses to a particular stimulus are generated by separate neurons, permitting the activation of different downstream pathways.^{1,22} In contrast, cells that produce both ON and OFF responses are likely to activate the same downstream neurons at stimulus onset and offset. We therefore asked whether individual bitter-sensing cells produce both ON and OFF responses. We used stochastic labeling and identified flies that contained a single labellar bitter neuron expressing GCaMP. All 15 cells that were imaged showed both ON and OFF responses to at least some bitter stimuli (Figure 2I). Thus, individual bitter cells produce both ON and OFF responses, implying that the same downstream pathways may be activated at the onset and offset of each stimulus.

Bitter response dynamics change with repeated taste presentation

In nature, flies are likely to taste a food source multiple times. We therefore tested whether bitter response dynamics change with repeated taste stimulation. We found that the ON response to denatonium habituated much more strongly than the OFF response (Figures 3A and 3B). With a 10 s interpulse interval (IPI), the ON response decayed by more than 85% within 3 presentations, whereas the OFF response decayed by less than 15%. By the fifth presentation, the ON response became negative (Figure 3B, top trace). Strong habituation of the ON

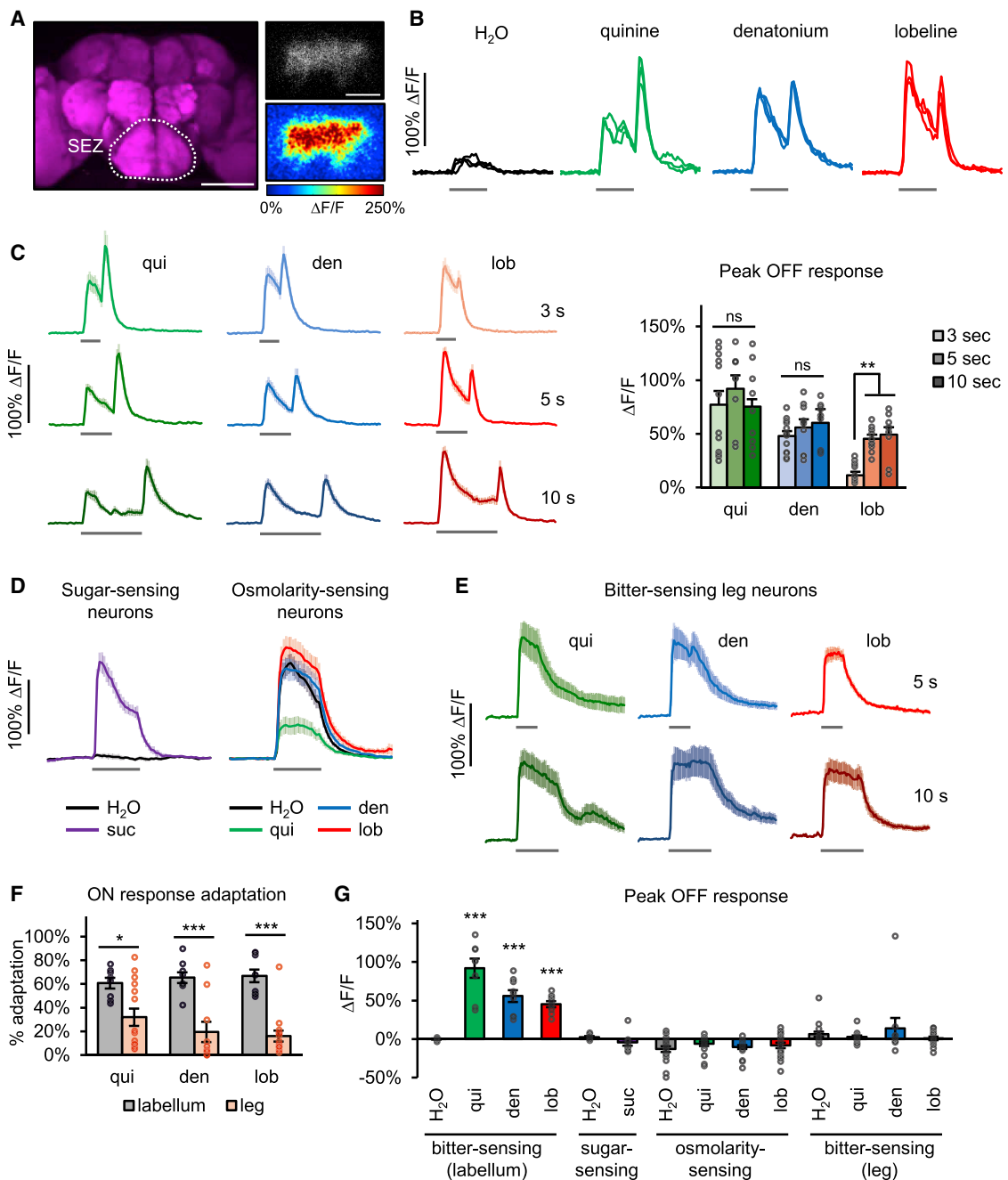


Figure 1. The timing of taste responses varies by modality and organ

(A) Left: location of the SEZ in the brain. Top right: bitter sensory axons expressing GCaMP are shown. Bottom right: heatmap of GCaMP response to denatonium (average over 3 trials) is shown. Scale bar, 100 μ m (left) and 20 μ m (upper right).

(B) Responses of labellar bitter-sensing neurons (individual trials from one fly).

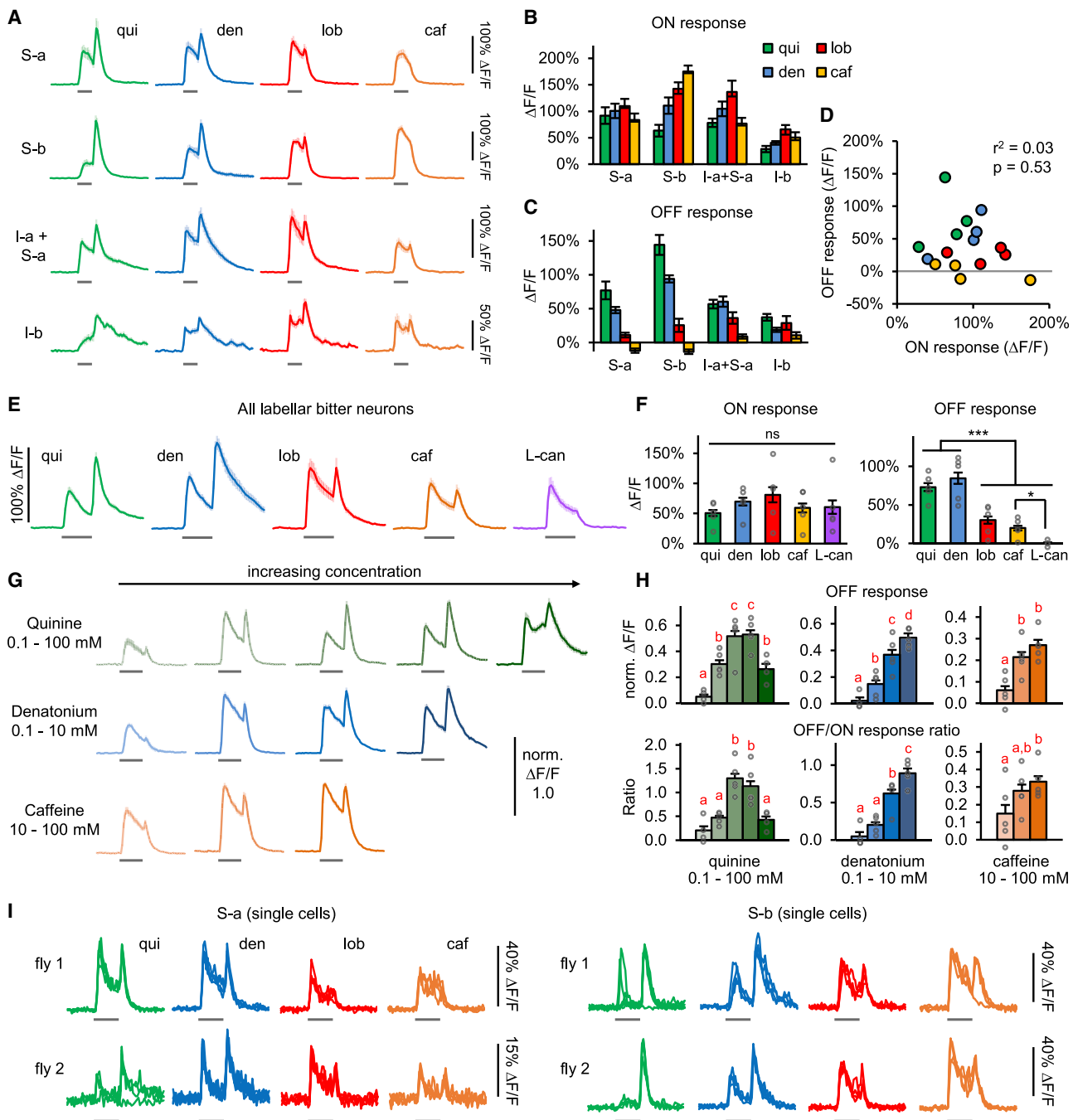
(C) Responses of labellar bitter-sensing neurons to 3, 5, or 10 s bitter stimulation ($n \geq 8$ trials, 3 flies). Left: average GCaMP traces are shown. Right: peak OFF response is shown (one-way ANOVA followed by Tukey's post-test).

(D) Responses of labellar sugar-sensing neurons ($n = 9$ trials, 3 flies) and osmolarity-sensing neurons ($n = 18$ trials, 6 flies).

(E) Responses of tarsal bitter-sensing neurons ($n \geq 9$ trials, 3–5 flies).

(F) ON response adaptation in labellar versus tarsal bitter neurons (t test).

(G) Peak OFF responses of different taste neurons (one-sample t test versus 0; only significant values greater than zero are noted). See also Figure S1. For all figures, * $p < 0.05$, ** $p < 0.01$, and *** $p < 0.001$. Graphs represent mean \pm SEM unless otherwise specified. Data points overlaid on bar graphs represent responses from individual trials (Figures 1 and 4) or flies (Figures 2, 3, 5, and 6). Gray bars denote stimulus presentation, and stimulus duration was 5 s unless otherwise specified. See STAR Methods for fly genotypes used.

**Figure 2. Further characterization of the bitter OFF response**

(A) Responses of labellar bitter neuron subsets to four bitter compounds ($n \geq 12$ trials, 4 flies). OFF responses appear less pronounced than in other figures because stimulus duration was 3 s instead of 5 s.

(B and C) Peak ON (B) and OFF (C) responses for data shown in (A). There was a significant effect of compound and class for both the ON and OFF response ($p < 0.0001$; two-way ANOVA).

(D) No correlation was observed between peak ON and OFF responses ($r^2 = 0.03$; $p = 0.53$; Pearson's correlation). Each point represents the average response of one neuronal class to one compound; points are colored by compound as in (A)–(C).

(E and F) Stimulus-dependent dynamics were observed when labeling all labellar bitter neurons ($n = 15$ trials, 5 flies).

(G) Responses of S-a bitter cells to varying bitter concentrations ($n \geq 12$ trials, 4 flies). See STAR Methods for concentrations used. $\Delta F/F$ values were normalized by fly to facilitate across-fly comparisons.

(H) Peak OFF response (top) and OFF/ON response ratio (bottom) for data from (G) (same legend colors).

(I) Responses of single bitter-sensing cells. Traces represent individual trials.

In (F) and (H), responses were compared by one-way ANOVA followed by Tukey's post-tests. In (H), bars labeled with different letters show a significant difference at $p < 0.05$. See also Figure S2.

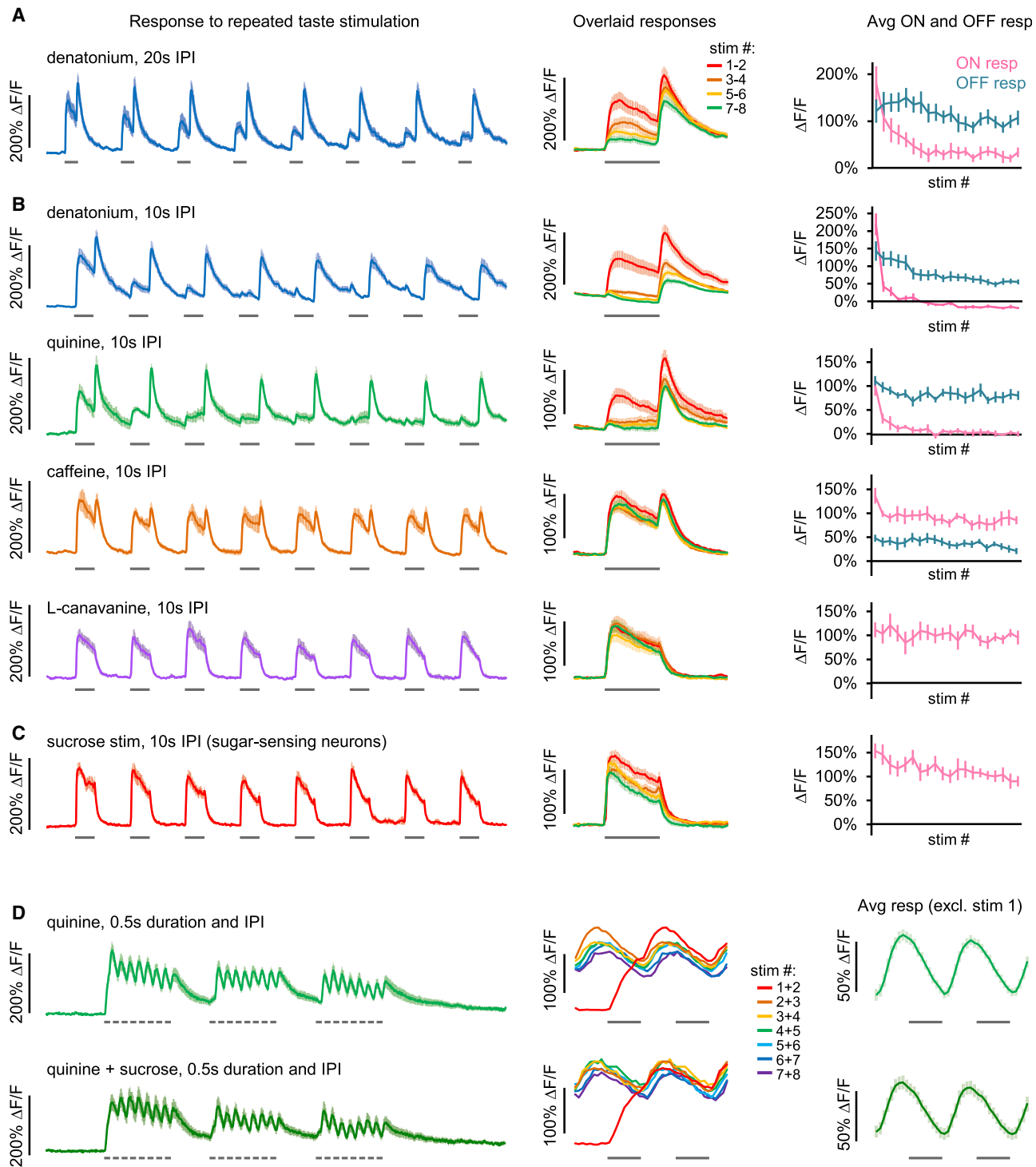


Figure 3. Bitter response dynamics change with repeated stimulus presentation

(A–C) Responses of labellar bitter-sensing (A and B) or sugar-sensing (C) neurons to 5 s stimuli delivered with a 20 s (A) or 10 s (B and C) IPI ($n = 6$ –8 flies). Left: average traces are shown. Middle: graphs show overlaid responses to different stimulus repetitions. Right: average ON and OFF responses to each stimulus repetition are shown.

(D) Response of labellar bitter neurons to 8×0.5 s stimuli with a 0.5 s IPI, repeated over 3 blocks with an interval of 5 s ($n = 9-10$ trials, 5 flies). Stimuli used were quinine (top) or quinine + sucrose (bottom). Left: average traces are shown. Middle: graphs show overlaid responses to two consecutive stimulus repetitions during the first block. Error bars are omitted for clarity. Right: graphs show average response to two consecutive stimulus repetitions, excluding the first stimulus of each block.

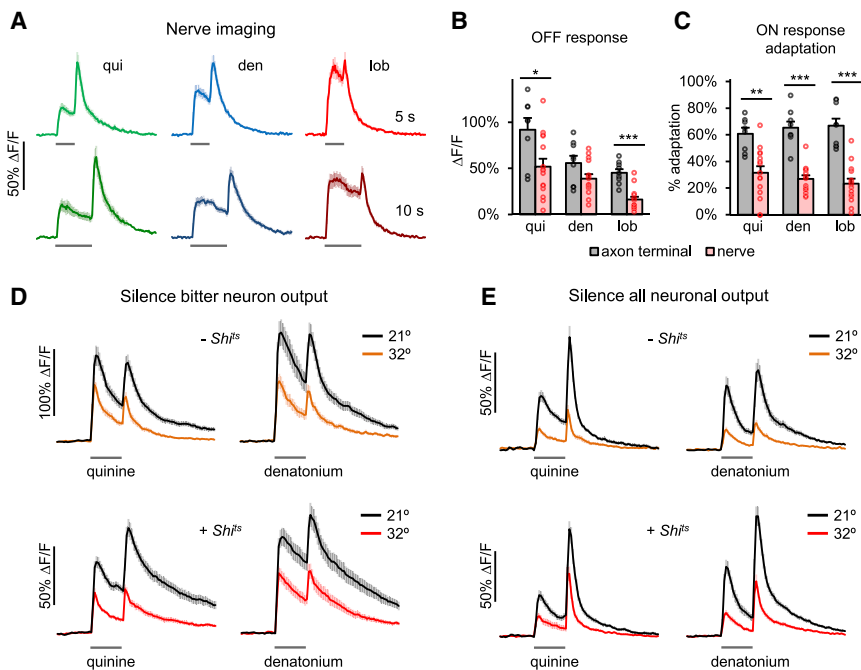


Figure 4. The bitter OFF response is generated cell intrinsically

(A) Responses of labellar bitter-sensing axons imaged in the labial nerve ($n \geq 14$ trials, 5 flies). Stimulation was 5 s or 10 s.

(B and C) Peak OFF response (B) and ON response adaptation (C) for labellar bitter neurons imaged in the nerve versus the SEZ (data from Figure 1C) with 5 s stimulation (Mann-Whitney test).

(D) Responses of bitter-sensing neurons when their synaptic output was silenced.

Control flies ($-Shi^{ts}$; $n = 16$ trials, 4 flies) were compared to experimental flies ($+Shi^{ts}$; $n \geq 28$ trials, 7 flies).

(E) Responses of bitter-sensing neurons when synaptic transmission was silenced pan-neuronally. Control flies ($-Shi^{ts}$; $n = 24$ trials, 6 flies) were compared to experimental flies ($+Shi^{ts}$; $n = 24$ trials, 6 flies).

response, but not the OFF response, was also observed with quinine (Figure 3B). Interestingly, strong ON response habituation was not observed with caffeine and L-canavanine, bitter stimuli that produce weaker or no OFF responses (Figure 3B), nor was it observed in sugar-sensing neurons (Figure 3C).

The natural feeding pattern of flies includes brief, repeated labellar contacts that can occur on a sub-second time-scale.^{33,34} We mimicked this pattern of taste stimulation by delivering a sequence of 0.5 s quinine stimuli with a 0.5 s IPI, repeated over three blocks (Figure 3D, top). On the first stimulus of each block, bitter onset led to an increase in activity that was further increased at bitter offset (Figure 3D, top center), consistent with our previous results (Figures 1 and 2). However, subsequent stimuli elicited a decrease in activity upon bitter onset and an increase at bitter offset. Thus, the GCaMP signal tracks the bitter stimulus, but in contrast to a typical sensory response, increasing activity corresponds to the absence of bitter, whereas decreasing activity corresponds to its presence (Figure 3D). Presenting the same stimulation pattern with sucrose added to quinine, representing a more natural food source, elicited similar dynamics as quinine alone (Figure 3D, bottom). These results show that, in a fly repeatedly sampling a bitter-containing substrate, which may represent natural feeding behavior, the OFF response rather than the ON response drives increases in bitter neuron activity.

Bitter OFF responses are generated cell-intrinsically

We tested whether the bitter OFF response is generated cell-intrinsically or through a circuit mechanism. Synaptic inputs onto the dendrites of labellar taste neurons have not been reported, but their axon terminals may receive modulatory inputs.^{35–37} Thus, if the OFF response is generated by a circuit mechanism, it should not be observed upstream of the axon terminals. We imaged bitter neuron axons in the labial nerve before

they enter the brain and observed strong ON and OFF responses (Figures 4A–4C), suggesting that the OFF response is generated cell-intrinsically. Nerve responses showed smaller OFF responses and less ON response adaptation than

the axon terminals (Figures 4A–4C), implying that some aspects of the response may be affected by modulation at the axon terminals.

We next silenced synaptic transmission from the bitter neurons to test the possibility of a feedback circuit mechanism that could generate the OFF response. We used the temperature-sensitive dynamin allele *Shibire^{ts}* (*Shi^{ts}*).³⁸ which blocks synaptic transmission at high temperatures. Bitter ON and OFF responses were generally diminished at 32° in both control and experimental flies, reflecting a suppressive effect of high temperature, but the two groups of flies did not differ in their dynamics (Figure 4D). We also imaged the responses of bitter neurons while silencing synaptic transmission in all brain neurons. When flies of this genotype were transferred to 32°, they were completely paralyzed, demonstrating the efficacy of synaptic silencing. However, bitter neurons in these flies continued to show both ON and OFF responses at 32° (Figure 4E). These results demonstrate that bitter OFF responses persist in the absence of synaptic transmission and likely result from cell-intrinsic mechanisms.

OFF responses in bitter neurons are generated by bitter receptors

We then examined whether the OFF response is generated by bitter receptors or results from a more general property of the sensory neuron (Figure 5A). We first tested whether an OFF response is generated following optogenetic activation of the bitter neurons using the light-activated cation channel Chrimson.³⁹ Chrimson-expressing bitter neurons were activated by light but failed to produce an OFF response when the light was turned off (Figure 5B), indicating that the OFF response is not a general consequence of neuronal depolarization.

We next asked whether known bitter receptors are required for the OFF response. Each labellar bitter neuron expresses

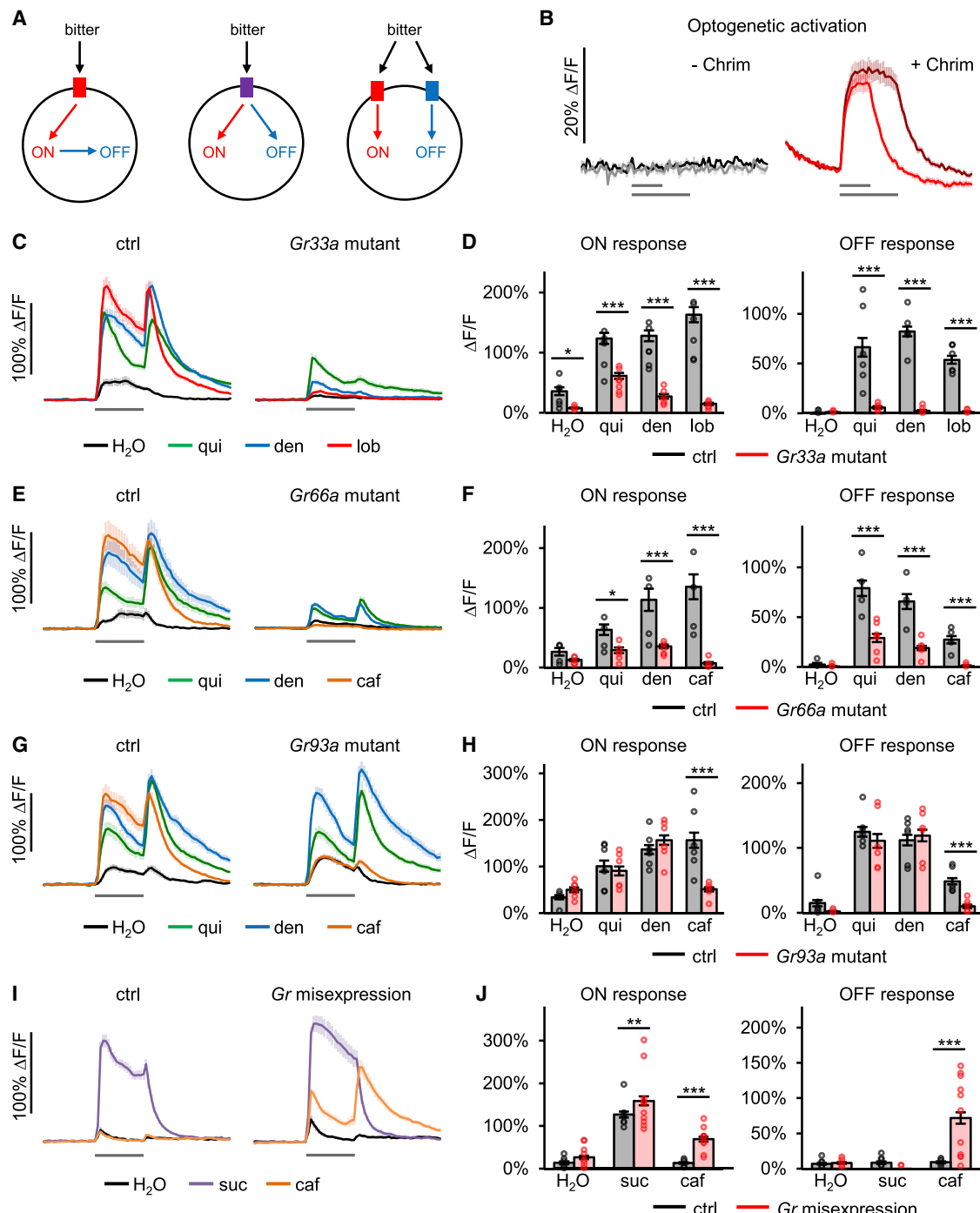


Figure 5. OFF responses in bitter-sensing neurons are generated by the same receptors that produce ON responses

(A) The OFF response could reflect a general mechanism producing rebound excitation following depolarization (left) or could require bitter ligands to bind specific receptors. In the latter case, ON and OFF responses could be generated by the same receptor (center) or different receptors (right).

(B) Responses of labellar bitter-sensing neurons to optogenetic activation. Control flies ("– Chrim"; n = 4 trials, 2 flies) were compared to experiments ("+ Chrim"; n = 21 trials, 7 flies). Chrimson-expressing neurons also showed a response to the two-photon laser.

(C–H) Bitter responses in flies carrying mutations in *Gr33a* (C and D), *Gr66a* (E and F), or *Gr93a* (G and H) were compared to responses in heterozygous controls (n ≥ 12 trials, 4–7 flies).

(I and J) Responses of sugar-sensing neurons expressing four caffeine receptor subunits were compared to control sugar neurons (n ≥ 28 trials, 7–11 flies). Sucrose responses were tested as a positive control.

Genotypes were compared by two-way ANOVA followed by Bonferroni post-tests. See also Figure S3.

between 6 and 28 bitter receptor subunits that form heteromeric receptor complexes.^{32,40–42} We first tested flies carrying mutations in *Gr33a* or *Gr66a*, broadly expressed subunits required for responses to many different compounds.^{42,43} Both *Gr33a* and *Gr66a* mutants showed impaired ON and OFF responses to all bitter compounds tested (Figures 5C–5F). We next tested flies carrying a mutation in *Gr93a*, a subunit required for detecting a small subset of bitter compounds, including caffeine.^{40,42} In *Gr93a* mutant flies, the ON and OFF responses to caffeine were severely impaired, whereas responses to quinine and denatonium were not affected (Figures 5G and 5H). Thus, different bitter compounds elicit OFF responses through different receptors, whereas the same receptor subunit is required for the ON and OFF response to a given compound.

We used misexpression experiments to test whether ON and OFF responses to caffeine are generated by a single receptor complex or two different complexes (Figure 5A, center versus right model). Misexpression of four receptor subunits (*Gr33a*, *Gr66a*, *Gr93a*, and *Gr39a.a*) in sugar-sensing neurons was shown to confer an ON response to caffeine.⁴² All four subunits are required for the ON response, suggesting that they form a single receptor complex.^{42,43} We repeated this experiment and found that expressing these four subunits in sugar-sensing neurons conferred both an ON and OFF response to caffeine (Figures 5I and 5J). These results suggest that a single receptor complex generates both the ON and OFF responses to a given bitter compound.

How could a single receptor complex generate both an ON and OFF response? Bitter taste receptors in insects are thought to be ligand-gated ion channels.⁴¹ In one model, ligand binding opens the receptor, which gradually becomes inactivated (Figures S3A and S3B).⁴⁴ Release of the ligand may relieve inactivation, allowing the channel to produce an OFF response before closing. The gradual inactivation of the receptor could also explain the strong adaptation of the ON response (Figure 1). We built a computational model of this mechanism (STAR Methods) and found that it generated ON and OFF responses that resembled the experimental data (Figures S3C and S3D). Changing a few parameters of the model resulted in varying dynamics that could mimic ligand-specific responses (Figure S3E). We also modeled habituation with repeated bitter stimulation. We postulated that habituation reflects each receptor shifting into a conformation that produces less output, and the habituated conformation may differ depending on whether bitter is bound (Figure S3F). The model was able to generate stronger habituation of the ON response than the OFF response (Figure S3F), recapitulating the data. Together, these studies suggest how receptor inactivation could enable a single receptor to generate both an ON and OFF response with different properties.

Bitter ON and OFF responses are propagated to downstream dopaminergic neurons

We next examined whether ON and OFF responses can be observed in neurons downstream of bitter sensory cells. Bitter signals are transmitted to the PPL1 subset of dopaminergic neurons (DANs),^{45,46} which respond to aversive stimuli and innervate the mushroom body, the learning and memory center of the fly.⁴⁷ Four of the five PPL1 DANs innervating the mushroom body

responded to labellar bitter stimulation, as previously reported,⁴⁵ and they showed both ON and OFF responses (Figures 6A–6D, S4A, and S4B). In contrast, applying bitter stimuli to the leg elicited an ON response but no OFF response (Figures 6B and 6C). PPL1 DANs showed similar ligand- and experience-dependent dynamics (Figures 6D, 6E, and S4C) as labellar bitter sensory neurons (Figures 2E, 3A, and 3B). Bitter response dynamics in the PPL1 DANs were not modulated by hunger or the presence of sugar (Figures S4D and S4E), similar to results in sensory neurons (Figures S2F and S2G). We also imaged taste responses in PAM DANs, which encode rewarding stimuli.⁴⁷ The PAM $\gamma 4$ DAN responded reliably to sugar and water but showed very weak and inconsistent responses to bitter (Figure S4F). The fact that reward-encoding DANs are not activated by the bitter OFF response argues against the possibility that it represents a “relief from punishment” signal that conveys an attractive valence.

Pairing odor and bitter induces unexpected effects on MBON plasticity

The timing of PPL1 DAN activity influences synaptic plasticity during aversive learning, in which an odor (the conditioned stimulus [CS]) is paired with a punishment (the unconditioned stimulus [US]). Odor-responsive Kenyon cells (KCs) synapse onto mushroom body output neurons (MBONs), and US-responsive PPL1 DANs modulate the strength of synapses onto MBONs that promote attraction (Figure 7A).^{48–50} During aversive conditioning, the simultaneous presentation of an odor with a punishment leads to coincident activation of KCs and PPL1 DANs, which induces depression at active KC-MBON synapses and results in odor avoidance.^{51,52} In contrast, DAN activation prior to odor delivery or in the absence of odor induces MBON facilitation.^{21,52,53}

Labellar bitter stimulation presents an interesting problem: a bitter US will evoke both an ON and OFF response in the DANs, but the OFF response is not coincident with bitter. If bitter is paired with odor using a typical aversive learning protocol, in which odor predicts bitter onset and terminates at or before bitter offset, the odor will overlap with the bitter ON response, but not the OFF response (Figure 7B, top). Conversely, if bitter is presented first and odor predicts bitter removal (Figure 7B, bottom), representing a typical “relief learning” paradigm,¹⁹ then odor will overlap with the bitter OFF response, but not the ON response. In each case, one peak of DAN activity coincides with odor while the other does not, suggesting that the two peaks may drive plasticity in opposite directions. The bitter ON and OFF responses in the DAN thus raise an intriguing question of the nature of the plasticity observed when bitter is used as a reinforcement cue. We chose to use repeated odor-bitter pairings because otherwise the pairing would be quite brief relative to other odor learning paradigms,^{54–57} and pilot experiments with a single pairing did not reveal any MBON plasticity (data not shown). Repeatedly pairing odor and bitter predicts that the plasticity driven by the bitter OFF response may be the dominant effect because the ON response preferentially habituates during repeated bitter presentation (Figures 6E and S4C).

We first paired odor with bitter onset, representing a typical aversive learning protocol (Figure 7B, top). MBON plasticity was examined by comparing the response of the $\gamma 2\alpha'1$ MBON

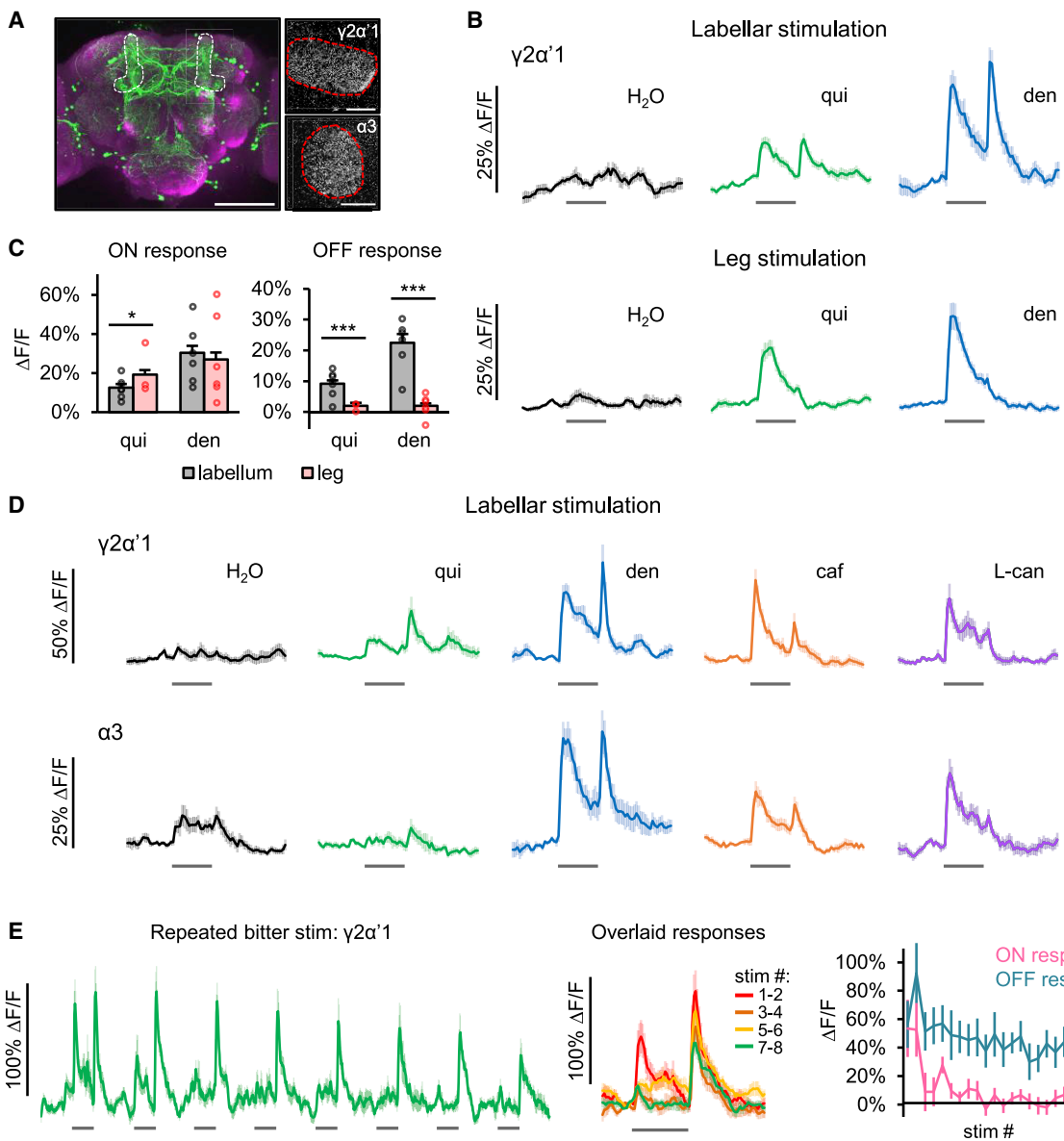


Figure 6. Bitter ON and OFF responses are propagated to PPL1 DANs

(A) PPL1 DANs were targeted by *TH-Gal4*. Left: image shows *TH-Gal4* expression pattern in a fixed and stained brain. The vertical lobes of the mushroom body containing PPL1 DAN axons are circled. Right: images show example frames from GCaMP imaging of $\gamma 2\alpha'1$ or $\alpha 3$ DAN axons in the mushroom body (maximum projections of 10–20 frames). Scale bars, 100 μm (left) and 20 μm (right).

(B) Responses of $\gamma 2\alpha'1$ DAN to bitter stimulation of the labellum ($n \geq 23$ trials, 7 cells in 4 flies) or the leg ($n \geq 26$ trials, 3–6 flies).

(C) Peak ON and OFF responses of the $\gamma 2\alpha'1$ DAN (Mann-Whitney test).

(D) Responses of $\gamma 2\alpha'1$ and $\alpha 3$ DANs to labellar stimulation with different bitter compounds ($n = 12$ trials, 4 flies).

(E) Response of the $\gamma 2\alpha'1$ DAN to repeated denatonium delivered with a 10 s IPI ($n = 9$ flies). Left: average GCaMP traces are shown. Middle: graphs show overlaid responses to different stimulus repetitions. Right: average ON and OFF responses to each stimulus repetition are shown.

See also Figure S4.

(Figure 7C) to the conditioned odor (CS+) before and after pairing. As a control, we repeated the same protocol for a different odor (the unconditioned odor, CS-) without bitter pairing (“mock pairing”). We noted that the MBON response to the CS- decreased with repeated presentations, representing odor habituation (Figure 7D). The effect of odor-bitter pairing was quantified by comparing the change in the CS+ and CS-

responses after pairing or mock pairing. Whereas pairing an odor with an aversive US normally induces MBON depression,^{21,53,58} pairing odor with bitter enhanced the MBON response (Figures 7D–7F; compare CS+ to CS-). Pairing odor with water instead of bitter did not induce MBON plasticity (Figure S5C), consistent with our observation that water does not activate the $\gamma 2\alpha'1$ DAN (Figure 6D).

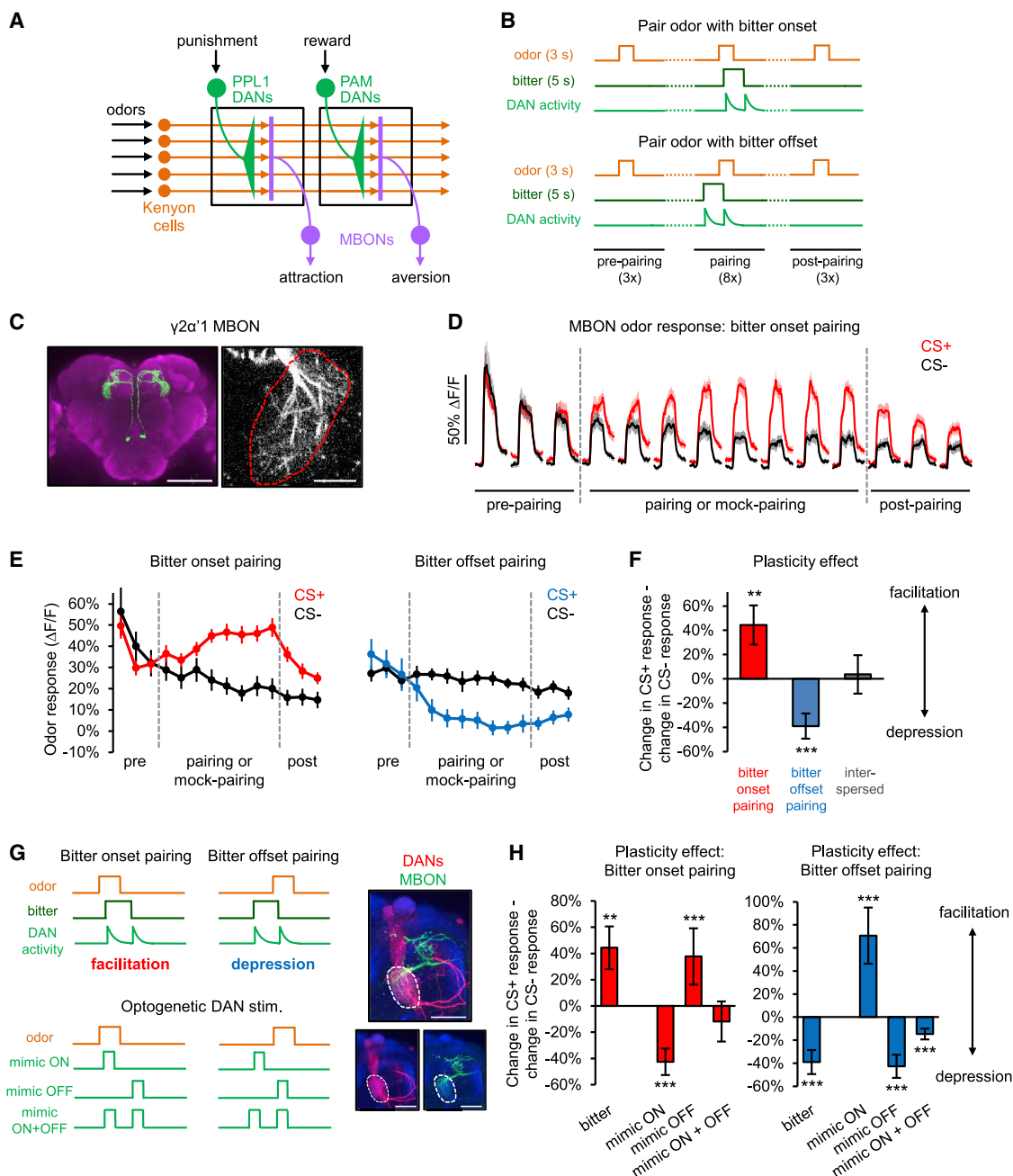


Figure 7. The OFF response drives MBON plasticity during odor-bitter pairing

(A) Schematic of the mushroom body circuit.

(B) Schematic of odor-bitter pairing experiments.

(C) $\gamma 2\alpha'1$ MBON labeled with the split *Ga4* line *MB077C*. Left: fixed and stained brain is shown. Right: example frame from GCaMP imaging is shown. $\gamma 2\alpha'1$ MBON dendrites are circled. Scale bars, 100 μ m (left) and 30 μ m (right).

(D) GCaMP responses of the $\gamma 2\alpha'1$ MBON to CS+ and CS- odors before, during, and after pairing with bitter onset (for the CS+) or mock pairing (for the CS-; n = 5 flies, 15 blocks).

(E) Average odor response of the $\gamma 2\alpha'1$ MBON during bitter onset (n = 5 flies, 15 blocks) and bitter offset (n = 7 flies, 21 blocks) pairing protocols.

(F) MBON plasticity induced by each pairing protocol (n \geq 5 flies, 15 blocks).

(G) Left: optogenetic stimulation of the $\gamma 2\alpha'1$ DAN was timed to mimic the bitter ON and/or OFF response in each pairing protocol. Right: images show expression of drivers used for optogenetic experiments, with $\gamma 2\alpha'1$ DAN labeled with the split *Ga4* line *MB099C* and $\gamma 2\alpha'1$ MBON labeled with *25D01-lexA*. The $\gamma 2\alpha'1$ compartment is outlined. Scale bars: 30 μ m.

(H) MBON plasticity induced by each optogenetic pairing protocol (n = 6–8 flies, 18–24 blocks).

In (F) and (H), error bars represent standard deviation obtained by bootstrapping, and p values were obtained by permutation testing. See also Figure S5.

We next paired odor with bitter offset, representing a typical relief learning or “backward pairing” protocol in which the US precedes the CS (Figure 7B, bottom). Backward pairing using electric shock as the US induces MBON facilitation,²¹ but when we used bitter as the US, we observed MBON depression (Figures 7E and 7F). No MBON plasticity was observed when odor and bitter stimuli were interspersed (Figure 7F). These results demonstrate that pairing odor with bitter onset versus bitter offset leads to opposing effects on MBON plasticity, and both effects contrast with previous results using other aversive USs.

The bitter OFF response drives plasticity during repeated odor-bitter pairing

The presence of a bitter OFF response in the DAN might explain why the plasticity effects we observe differ from results obtained with other aversive USs. In particular, the plasticity effects in our experiments may be primarily driven by the OFF response because we paired odor and bitter 8 times, and with repeated bitter stimulation, the ON response habituates much more strongly than the OFF response (Figure 6E). We tested this hypothesis by performing pairing experiments in which we replaced bitter with optogenetic stimulation of the $\gamma 2\alpha'1$ DAN. We stimulated the DAN to mimic the timing of the bitter ON response, the OFF response, or both the ON and OFF responses and asked which protocol reproduces the effects of bitter pairing (Figures 7G and 7H).

We first employed photostimulation to mimic the protocol in which odor is paired with bitter onset, which induces MBON facilitation. When we mimicked only the ON response, such that the DAN is only activated during odor presentation, we observed MBON depression (Figures 7G and 7H). In contrast, mimicking the timing of the OFF response, such that the DAN is activated after odor removal, resulted in MBON facilitation (Figures 7G and 7H). Mimicking both the ON and OFF response did not induce significant plasticity (Figures 7G and 7H). These experiments suggest that, in this paradigm, the bitter ON and OFF responses induce opposing forms of MBON plasticity, and the facilitation driven by the OFF response is the dominant effect that is observed.

We next mimicked the protocol in which odor is paired with bitter offset, which induces MBON depression. Optogenetically mimicking the timing of the ON response resulted in MBON facilitation, whereas mimicking the timing of the OFF response led to MBON depression (Figures 7G and 7H). Mimicking both the ON and OFF response led to very weak MBON depression (Figures 7G and 7H). Thus, in this paradigm, the bitter ON and OFF responses induce opposing types of plasticity, and the depression driven by the OFF response dominates. Together, these results demonstrate that repeatedly pairing odor with either bitter onset or offset leads to opposite effects on MBON plasticity than is observed with other aversive USs, and these effects can be explained by the bitter OFF response.

DISCUSSION

We found that bitter neurons in the labellum display both ON and OFF responses, whereas neurons activated by other tastants exhibit only an ON response. The ON and OFF responses result from cell-intrinsic mechanisms, and a single receptor complex likely generates both the ON and OFF responses to a given

compound. The bitter ON and OFF responses in sensory neurons are propagated downstream to PPL1 DANs, which mediate synaptic plasticity. Repeatedly pairing odor with bitter onset versus bitter offset led to opposing effects on MBON plasticity, and both effects contrasted with the types of plasticity that have been observed using other aversive USs. Optogenetic experiments suggested that this difference is due to the presence of the bitter OFF response. Together, these studies identify ON and OFF responses in individual bitter neurons and reveal their influence on neural circuit function.

Bitter OFF responses in the labellum

The strong OFF response we observe has not been previously described in studies of *Drosophila* bitter neurons. This may reflect methodological differences. Electrophysiological recordings of taste neurons typically use a technique that precludes neural recordings after stimulus removal.^{32,42,43,59} Calcium imaging studies did not monitor the response after bitter offset,⁶⁰ delivered bitter tastants through a continuous liquid flow without precise control of bitter offset,⁶¹ or used bitter compounds or concentrations that may not lead to a strong OFF response.^{35,37,62} However, a recent study describes OFF responses in bitter sensory neurons and their postsynaptic partners.⁶³ In addition, OFF responses were noted in DANs stimulated with quinine.⁶⁴

Our experiments suggest that the OFF response is generated by bitter receptors rather than resulting from circuit mechanisms or general depolarization of the cell. Misexpression of four sub-units composing the caffeine receptor confers both ON and OFF responses to caffeine, suggesting that a single receptor generates both ON and OFF responses to a given compound. This contrasts with recently described ON and OFF responses to lactic acid in sugar-sensing neurons, which are mediated by different receptors.⁶⁵ We suggest a model in which the bitter receptor opens upon ligand binding and then inactivates, leading to adaptation of the ON response; ligand release relieves inactivation and generates an OFF response. Computational modeling of this mechanism simulated ON and OFF responses that resembled the experimental data. However, alternative mechanisms are also possible. For example, receptor output could be suppressed by an inhibitory feedback pathway rather than intrinsic inactivation, resulting in an OFF response if the inhibition terminates more quickly than the channel closes.

Bitter ON and OFF responses influence synaptic plasticity

The observation that individual neurons produce both ON and OFF responses has implications for timing-based synaptic plasticity, which underlies associative learning across many systems.^{66,67} In flies, associative learning depends on synaptic plasticity induced by coincident activation of CS- and US-responsive neurons.^{51,52} An OFF response leads to a temporal dissociation between the presence of a stimulus and the neuron’s activation, because the neuron is activated after the stimulus is removed, suggesting that an OFF response could alter plasticity during associative learning. Our experiments reveal that this is the case. Repeated pairing of odor with bitter onset or offset results in MBON plasticity effects that contrast with the sign of plasticity induced by other aversive USs.^{21,53,58} We have not determined whether the learned behavior is also

reversed. Our odor-bitter pairing experiments were designed to test whether the bitter OFF response influences synaptic plasticity, not to mimic natural conditions. In nature, odor is unlikely to be repeatedly paired with only bitter onset or offset. Moreover, in nature, flies may simultaneously taste bitter with the legs and labellum, which could lead to different patterns of DAN activity.

Behavioral relevance of bitter ON and OFF responses

The appearance and disappearance of a stimulus have different meanings, and an organism would be expected to respond differently—potentially in opposite ways—to these two events. Generating ON and OFF responses in different neural pathways, as occurs in the visual system²² and the *C. elegans* olfactory system,^{17,18} enables the brain to generate different behavioral responses to stimulus onset and offset. However, bitter elicits both ON and OFF responses in the same sensory cells. One possibility is that the bitter ON and OFF responses activate common circuits to elicit similar behavioral effects. For example, both peaks of activity may act to suppress feeding, and perhaps this response is elicited at both bitter onset and offset to ensure that the fly continues to show aversion for several seconds after tasting bitter. Analogous to this model, both the ON and OFF responses to lactic acid in sugar-sensing neurons promote feeding attraction.⁶⁵ Alternatively, bitter ON and OFF responses may elicit different behavioral responses despite occurring in the same cells. This would provoke the question of how downstream pathways disambiguate the two responses. In support of this idea, the bitter ON and OFF responses are differentially sensitive to bitter identity, concentration, and repeated bitter exposure, suggesting that they may convey different types of information.

Any hypotheses regarding the behavioral role of the bitter OFF response must consider the observation that it occurs in labellar, but not tarsal, neurons. Tarsal taste neurons have been implicated in locomotor attraction to sugar²⁵ and aversion to bitter.²⁷ Tarsal bitter responses, which show a sustained ON response and no OFF response, may therefore be adapted for continuously reading out the bitter quality of the substrate to mediate locomotor repulsion. In contrast, labellar taste neurons are activated only when the fly extends its proboscis to sample or ingest food. The bitter OFF response would occur immediately after contact and may be behaviorally important during longer bouts of feeding. Continued feeding in the presence of bitter is unlikely to occur unless the substrate also contains an appetitive tastant, such as sugar. Adaptation of the bitter ON response may enable appetitive pathways to more readily override bitter-induced aversion, permitting the fly to continue feeding. Similarly, during repeated food contacts, the bitter ON response may habituate to enable the fly to continue feeding despite the presence of bitter. The OFF response may inform the fly of the presence of bitter once feeding has terminated. This signal could be used to suppress further feeding bouts, promote locomotion to a better food source, or serve as a US that reinforces aversive learning. In this manner, the bitter OFF response may elicit adaptive behaviors or reinforce memory following the consumption of aversive bitter stimuli.

STAR★METHODS

Detailed methods are provided in the online version of this paper and include the following:

- KEY RESOURCES TABLE
- RESOURCE AVAILABILITY
 - Lead contact
 - Materials availability
 - Data and code availability
- EXPERIMENTAL MODEL AND SUBJECT DETAILS
 - Fly strains and maintenance
 - Fly genotypes for each experiment
- METHOD DETAILS
 - Taste stimulation and calcium imaging
 - Single cell labeling
 - Shibire silencing
 - Optogenetic stimulation
 - Odor-bitter pairing
 - Immunohistochemistry
 - Computational modeling of receptor function
- QUANTIFICATION AND STATISTICAL ANALYSIS
 - Calcium imaging analysis
 - Statistical testing
 - Decoding analysis

SUPPLEMENTAL INFORMATION

Supplemental information can be found online at <https://doi.org/10.1016/j.cub.2021.10.020>.

ACKNOWLEDGMENTS

We thank Daisuke Hattori for assistance with calcium imaging and analysis code; Larry Abbott and Joel Butterwick for feedback on receptor modeling; Peter Wang for advice on decoder analyses; Barbara Noro and Chris Rodgers for general advice and comments; members of the Axel laboratory for helpful feedback and suggestions; Adriana Nemes, Phyllis Kisloff, Miriam Gutierrez, and Clayton Eccard for general laboratory and administrative support; and John Carlson, Ulrike Heberlein, Craig Montell, Kristin Scott, Janelia Research Campus, and the Bloomington Drosophila Stock Center (BDSC) for generously providing fly strains. This work was supported by the Howard Hughes Medical Institute (R.A.).

AUTHOR CONTRIBUTIONS

A.V.D. conceived the project, generated figures, and performed all calcium imaging, data analysis, and computational modeling. J.U.D. performed immunohistochemistry experiments and provided technical assistance in other areas. B.S. assisted with some MBON imaging experiments. R.A. supervised the project. A.V.D. and R.A. wrote the manuscript.

DECLARATION OF INTERESTS

The authors declare no competing interests.

Received: March 31, 2021

Revised: September 4, 2021

Accepted: October 8, 2021

Published: November 2, 2021

REFERENCES

1. Hubel, D.H., and Wiesel, T.N. (1961). Integrative action in the cat's lateral geniculate body. *J. Physiol.* **155**, 385–398.
2. Xu, N., Fu, Z.-Y., and Chen, Q.-C. (2014). The function of offset neurons in auditory information processing. *Transl. Neurosci.* **5**, 275–285.
3. Abraira, V.E., and Ginty, D.D. (2013). The sensory neurons of touch. *Neuron* **79**, 618–639.

4. Luo, M., and Katz, L.C. (2001). Response correlation maps of neurons in the mammalian olfactory bulb. *Neuron* 32, 1165–1179.
5. Sato, T. (1976). Off-response of gustatory nerve following termination of quinine stimuli applied to the frog tongue. *Chem. Sens.* 2, 63–69.
6. Qin, L., Chimoto, S., Sakai, M., Wang, J., and Sato, Y. (2007). Comparison between offset and onset responses of primary auditory cortex ON-OFF neurons in awake cats. *J. Neurophysiol.* 97, 3421–3431.
7. Scholl, B., Gao, X., and Wehr, M. (2010). Nonoverlapping sets of synapses drive on responses and off responses in auditory cortex. *Neuron* 65, 412–421.
8. Nagel, K.I., and Wilson, R.I. (2016). Mechanisms underlying population response dynamics in inhibitory interneurons of the Drosophila antennal lobe. *J. Neurosci.* 36, 4325–4338.
9. Pei, Y.C., Denchev, P.V., Hsiao, S.S., Craig, J.C., and Bensmaia, S.J. (2009). Convergence of submodality-specific input onto neurons in primary somatosensory cortex. *J. Neurophysiol.* 102, 1843–1853.
10. Gjorgjeva, J., Sompolinsky, H., and Meister, M. (2014). Benefits of pathway splitting in sensory coding. *J. Neurosci.* 34, 12127–12144.
11. Liang, Z., Shen, W., Sun, C., and Shou, T. (2008). Comparative study on the offset responses of simple cells and complex cells in the primary visual cortex of the cat. *Neuroscience* 156, 365–373.
12. Bregman, A.S., Ahad, P.A., and Kim, J. (1994). Resetting the pitch-analysis system. 2. Role of sudden onsets and offsets in the perception of individual components in a cluster of overlapping tones. *J. Acoust. Soc. Am.* 96, 2694–2703.
13. Mazor, O., and Laurent, G. (2005). Transient dynamics versus fixed points in odor representations by locust antennal lobe projection neurons. *Neuron* 48, 661–673.
14. Kennedy, J.S., and Marsh, D. (1974). Pheromone-regulated anemotaxis in flying moths. *Science* 184, 999–1001.
15. van Breugel, F., and Dickinson, M.H. (2014). Plume-tracking behavior of flying Drosophila emerges from a set of distinct sensory-motor reflexes. *Curr. Biol.* 24, 274–286.
16. Álvarez-Salvado, E., Licata, A.M., Connor, E.G., McHugh, M.K., King, B.M., Stavropoulos, N., Victor, J.D., Crimaldi, J.P., and Nagel, K.I. (2018). Elementary sensory-motor transformations underlying olfactory navigation in walking fruit-flies. *eLife* 7, e37815.
17. Chalasani, S.H., Chronis, N., Tsunozaki, M., Gray, J.M., Ramot, D., Goodman, M.B., and Bargmann, C.I. (2007). Dissecting a circuit for olfactory behaviour in *Caenorhabditis elegans*. *Nature* 450, 63–70.
18. Larsch, J., Flavell, S.W., Liu, Q., Gordus, A., Albrecht, D.R., and Bargmann, C.I. (2015). A circuit for gradient climbing in *C. elegans* chemotaxis. *Cell Rep.* 12, 1748–1760.
19. Tanimoto, H., Heisenberg, M., and Gerber, B. (2004). Experimental psychology: event timing turns punishment to reward. *Nature* 430, 983.
20. Gerber, B., Yarali, A., Diegelmann, S., Wotjak, C.T., Pauli, P., and Fendt, M. (2014). Pain-relief learning in flies, rats, and man: basic research and applied perspectives. *Learn. Mem.* 21, 232–252.
21. Handler, A., Graham, T.G.W., Cohn, R., Morantte, I., Siliciano, A.F., Zeng, J., Li, Y., and Ruta, V. (2019). Distinct dopamine receptor pathways underlie the temporal sensitivity of associative learning. *Cell* 178, 60–75.e19.
22. Westheimer, G. (2007). The ON-OFF dichotomy in visual processing: from receptors to perception. *Prog. Retin. Eye Res.* 26, 636–648.
23. Liman, E.R., Zhang, Y.V., and Montell, C. (2014). Peripheral coding of taste. *Neuron* 81, 984–1000.
24. Scott, K. (2018). Gustatory processing in *Drosophila melanogaster*. *Annu. Rev. Entomol.* 63, 15–30.
25. Thoma, V., Knapik, S., Arai, S., Hartl, M., Kohsaka, H., Sirigrivatanawong, P., Abe, A., Hashimoto, K., and Tanimoto, H. (2016). Functional dissociation in sweet taste receptor neurons between and within taste organs of *Drosophila*. *Nat. Commun.* 7, 10678.
26. Corfas, R.A., Sharma, T., and Dickinson, M.H. (2019). Diverse food-sensing neurons trigger idiothetic local search in *Drosophila*. *Curr. Biol.* 29, 1660–1668.e4.
27. Joseph, R.M., and Heberlein, U. (2012). Tissue-specific activation of a single gustatory receptor produces opposing behavioral responses in *Drosophila*. *Genetics* 192, 521–532.
28. Yanagawa, A., Guigue, A.M., and Marion-Poll, F. (2014). Hygienic grooming is induced by contact chemicals in *Drosophila melanogaster*. *Front. Behav. Neurosci.* 8, 254.
29. Thistle, R., Cameron, P., Ghorayshi, A., Dennison, L., and Scott, K. (2012). Contact chemoreceptors mediate male-male repulsion and male-female attraction during *Drosophila* courtship. *Cell* 149, 1140–1151.
30. He, Z., Luo, Y., Shang, X., Sun, J.S., and Carlson, J.R. (2019). Chemosensory sensilla of the *Drosophila* wing express a candidate ionotropic pheromone receptor. *PLoS Biol.* 17, e2006619.
31. Cameron, P., Hiroi, M., Ngai, J., and Scott, K. (2010). The molecular basis for water taste in *Drosophila*. *Nature* 465, 91–95.
32. Weiss, L.A., Dahanukar, A., Kwon, J.Y., Banerjee, D., and Carlson, J.R. (2011). The molecular and cellular basis of bitter taste in *Drosophila*. *Neuron* 69, 258–272.
33. Flood, T.F., Iguchi, S., Gorczyca, M., White, B., Ito, K., and Yoshihara, M. (2013). A single pair of interneurons commands the *Drosophila* feeding motor program. *Nature* 499, 83–87.
34. Itskov, P.M., Moreira, J.M., Vinnik, E., Lopes, G., Safarik, S., Dickinson, M.H., and Ribeiro, C. (2014). Automated monitoring and quantitative analysis of feeding behaviour in *Drosophila*. *Nat. Commun.* 5, 4560.
35. LeDue, E.E., Mann, K., Koch, E., Chu, B., Dakin, R., and Gordon, M.D. (2016). Starvation-induced depotentiation of bitter taste in *Drosophila*. *Curr. Biol.* 26, 2854–2861.
36. Inagaki, H.K., Ben-Tabou de-Leon, S., Wong, A.M., Jagadish, S., Ishimoto, H., Barnea, G., Kitamoto, T., Axel, R., and Anderson, D.J. (2012). Visualizing neuromodulation in vivo: TANGO-mapping of dopamine signaling reveals appetite control of sugar sensing. *Cell* 148, 583–595.
37. Chu, B., Chui, V., Mann, K., and Gordon, M.D. (2014). Presynaptic gain control drives sweet and bitter taste integration in *Drosophila*. *Curr. Biol.* 24, 1978–1984.
38. Kitamoto, T. (2001). Conditional modification of behavior in *Drosophila* by targeted expression of a temperature-sensitive shibire allele in defined neurons. *J. Neurobiol.* 47, 81–92.
39. Klapoetke, N.C., Murata, Y., Kim, S.S., Pulver, S.R., Birdsey-Benson, A., Cho, Y.K., Morimoto, T.K., Chuong, A.S., Carpenter, E.J., Tian, Z., et al. (2014). Independent optical excitation of distinct neural populations. *Nat. Methods* 11, 338–346.
40. Lee, Y., Moon, S.J., and Montell, C. (2009). Multiple gustatory receptors required for the caffeine response in *Drosophila*. *Proc. Natl. Acad. Sci. USA* 106, 4495–4500.
41. Shim, J., Lee, Y., Jeong, Y.T., Kim, Y., Lee, M.G., Montell, C., and Moon, S.J. (2015). The full repertoire of *Drosophila* gustatory receptors for detecting an aversive compound. *Nat. Commun.* 6, 8867.
42. Dweck, H.K.M., and Carlson, J.R. (2020). Molecular logic and evolution of bitter taste in *Drosophila*. *Curr. Biol.* 30, 17–30.e3.
43. Moon, S.J., Lee, Y., Jiao, Y., and Montell, C. (2009). A *Drosophila* gustatory receptor essential for aversive taste and inhibiting male-to-male courtship. *Curr. Biol.* 19, 1623–1627.
44. Ulbricht, W. (2005). Sodium channel inactivation: molecular determinants and modulation. *Physiol. Rev.* 85, 1271–1301.
45. Kirkhart, C., and Scott, K. (2015). Gustatory learning and processing in the *Drosophila* mushroom bodies. *J. Neurosci.* 35, 5950–5958.
46. Kim, H., Kirkhart, C., and Scott, K. (2017). Long-range projection neurons in the taste circuit of *Drosophila*. *eLife* 6, e23386.

47. Modi, M.N., Shuai, Y., and Turner, G.C. (2020). The Drosophila mushroom body: from architecture to algorithm in a learning circuit. *Annu. Rev. Neurosci.* 43, 465–484.
48. Aso, Y., Hattori, D., Yu, Y., Johnston, R.M., Iyer, N.A., Ngo, T.T., Dionne, H., Abbott, L.F., Axel, R., Tanimoto, H., and Rubin, G.M. (2014). The neuronal architecture of the mushroom body provides a logic for associative learning. *eLife* 3, e04577.
49. Owald, D., and Waddell, S. (2015). Olfactory learning skews mushroom body output pathways to steer behavioral choice in Drosophila. *Curr. Opin. Neurobiol.* 35, 178–184.
50. Aso, Y., Sitaraman, D., Ichinose, T., Kaun, K.R., Vogt, K., Belliard-Guérin, G., Plaçais, P.Y., Robie, A.A., Yamagata, N., Schnaitmann, C., et al. (2014). Mushroom body output neurons encode valence and guide memory-based action selection in Drosophila. *eLife* 3, e04580.
51. Hige, T., Aso, Y., Modi, M.N., Rubin, G.M., and Turner, G.C. (2015). Heterosynaptic plasticity underlies aversive olfactory learning in Drosophila. *Neuron* 88, 985–998.
52. Cohn, R., Morantte, I., and Ruta, V. (2015). Coordinated and compartmentalized neuromodulation shapes sensory processing in Drosophila. *Cell* 163, 1742–1755.
53. Berry, J.A., Phan, A., and Davis, R.L. (2018). Dopamine neurons mediate learning and forgetting through bidirectional modulation of a memory trace. *Cell Rep.* 25, 651–662.e5.
54. Perisse, E., Yin, Y., Lin, A.C., Lin, S., Huettneroth, W., and Waddell, S. (2013). Different kenyon cell populations drive learned approach and avoidance in Drosophila. *Neuron* 79, 945–956.
55. Das, G., Klappenbach, M., Vrontou, E., Perisse, E., Clark, C.M., Burke, C.J., and Waddell, S. (2014). Drosophila learn opposing components of a compound food stimulus. *Curr. Biol.* 24, 1723–1730.
56. Berry, J.A., Cervantes-Sandoval, I., Chakraborty, M., and Davis, R.L. (2015). Sleep facilitates memory by blocking dopamine neuron-mediated forgetting. *Cell* 161, 1656–1667.
57. Aso, Y., and Rubin, G.M. (2016). Dopaminergic neurons write and update memories with cell-type-specific rules. *eLife* 5, e16135.
58. Perisse, E., Owald, D., Barnstedt, O., Talbot, C.B., Huettneroth, W., and Waddell, S. (2016). Aversive learning and appetitive motivation toggle feed-forward inhibition in the Drosophila mushroom body. *Neuron* 90, 1086–1099.
59. Hiroi, M., Meunier, N., Marion-Poll, F., and Tanimura, T. (2004). Two antagonistic gustatory receptor neurons responding to sweet-salty and bitter taste in Drosophila. *J. Neurobiol.* 61, 333–342.
60. Marella, S., Fischler, W., Kong, P., Asgarian, S., Rueckert, E., and Scott, K. (2006). Imaging taste responses in the fly brain reveals a functional map of taste category and behavior. *Neuron* 49, 285–295.
61. Inagaki, H.K., Panse, K.M., and Anderson, D.J. (2014). Independent, reciprocal neuromodulatory control of sweet and bitter taste sensitivity during starvation in Drosophila. *Neuron* 84, 806–820.
62. Jaeger, A.H., Stanley, M., Weiss, Z.F., Musso, P.Y., Chan, R.C., Zhang, H., Feldman-Kiss, D., and Gordon, M.D. (2018). A complex peripheral code for salt taste in Drosophila. *eLife* 7, e37167.
63. Snell, N.J., Fisher, J.D., Hartmann, G.G., Talay, M., and Barnea, G. (2020). Distributed representation of taste quality by second-order gustatory neurons in Drosophila. *bioRxiv*. <https://doi.org/10.1101/2020.11.10.377382>.
64. Siju, K.P., Štih, V., Aimon, S., Gjorgjeva, J., Portugues, R., and Grunwald-Kadow, I.C. (2020). Valence and state-dependent population coding in dopaminergic neurons in the fly mushroom body. *Curr. Biol.* 30, 2104–2115.e4.
65. Stanley, M., Ghosh, B., Weiss, Z.F., Christiaanse, J., and Gordon, M.D. (2021). Mechanisms of lactic acid gustatory attraction in Drosophila. *Curr. Biol.* 31, 3525–3537.e6.
66. Feldman, D.E. (2012). The spike-timing dependence of plasticity. *Neuron* 75, 556–571.
67. Magee, J.C., and Grienberger, C. (2020). Synaptic plasticity forms and functions. *Annu. Rev. Neurosci.* 43, 95–117.
68. Scott, K., Brady, R., Jr., Cravchik, A., Morozov, P., Rzhetsky, A., Zuker, C., and Axel, R. (2001). A chemosensory gene family encoding candidate gustatory and olfactory receptors in Drosophila. *Cell* 104, 661–673.
69. Dahanukar, A., Lei, Y.T., Kwon, J.Y., and Carlson, J.R. (2007). Two Gr genes underlie sugar reception in Drosophila. *Neuron* 56, 503–516.
70. Jonson, M., Pokrzywa, M., Starkenberg, A., Hammarstrom, P., and Thor, S. (2015). Systematic A β analysis in Drosophila reveals high toxicity for the 1-42, 3-42 and 11-42 peptides, and emphasizes N- and C-terminal residues. *PLoS ONE* 10, e0133272.
71. Friggi-Grelin, F., Coulom, H., Meller, M., Gomez, D., Hirsh, J., and Birman, S. (2003). Targeted gene expression in Drosophila dopaminergic cells using regulatory sequences from tyrosine hydroxylase. *J. Neurobiol.* 54, 618–627.
72. Liu, C., Plaçais, P.Y., Yamagata, N., Pfeiffer, B.D., Aso, Y., Friedrich, A.B., Siwanowicz, I., Rubin, G.M., Prent, T., and Tanimoto, H. (2012). A subset of dopamine neurons signals reward for odour memory in Drosophila. *Nature* 488, 512–516.
73. Pfeiffer, B.D., Ngo, T.T., Hibbard, K.L., Murphy, C., Jenett, A., Truman, J.W., and Rubin, G.M. (2010). Refinement of tools for targeted gene expression in Drosophila. *Genetics* 186, 735–755.
74. Chen, T.W., Wardill, T.J., Sun, Y., Pulver, S.R., Renninger, S.L., Baohan, A., Schreiter, E.R., Kerr, R.A., Orger, M.B., Jayaraman, V., et al. (2013). Ultrasensitive fluorescent proteins for imaging neuronal activity. *Nature* 499, 295–300.
75. Barolo, S., Castro, B., and Posakony, J.W. (2004). New Drosophila transgenic reporters: insulated P-element vectors expressing fast-maturing RFP. *Biotechniques* 36, 436–440, 442.
76. Duistermars, B.J., Pfeiffer, B.D., Hooper, E.D., and Anderson, D.J. (2018). A brain module for scalable control of complex, multi-motor threat displays. *Neuron* 100, 1474–1490.e4.
77. Hattori, D., Aso, Y., Swartz, K.J., Rubin, G.M., Abbott, L.F., and Axel, R. (2017). Representations of novelty and familiarity in a mushroom body compartment. *Cell* 169, 956–969.e17.
78. Moon, S.J., Köttgen, M., Jiao, Y., Xu, H., and Montell, C. (2006). A taste receptor required for the caffeine response in vivo. *Curr. Biol.* 16, 1812–1817.
79. Nern, A., Pfeiffer, B.D., Svoboda, K., and Rubin, G.M. (2011). Multiple new site-specific recombinases for use in manipulating animal genomes. *Proc. Natl. Acad. Sci. USA* 108, 14198–14203.
80. Gordon, M.D., and Scott, K. (2009). Motor control in a Drosophila taste circuit. *Neuron* 61, 373–384.
81. Devineni, A.V., Sun, B., Zhukovskaya, A., and Axel, R. (2019). Acetic acid activates distinct taste pathways in *Drosophila* to elicit opposing, state-dependent feeding responses. *eLife* 8, e47677.
82. Wang, J.W., Wong, A.M., Flores, J., Vosshall, L.B., and Axel, R. (2003). Two-photon calcium imaging reveals an odor-evoked map of activity in the fly brain. *Cell* 112, 271–282.

STAR★METHODS

KEY RESOURCES TABLE

REAGENT or RESOURCE	SOURCE	IDENTIFIER
Antibodies		
Chicken anti-GFP	Aves Labs	Cat# GFP-1020; RRID:AB_10000240
Rabbit anti-DsRed	Clontech	Cat# 632496; RRID:AB_10013483
Mouse anti-bruchpilot (nc82)	Development Studies Hybridoma Bank	Cat# nc82; RRID:AB_2314866
Alexa Fluor 488 goat anti-chicken	Life Technologies	Cat# A11039; RRID:AB_2534096
Alexa Fluor 568 goat anti-rabbit	Life Technologies	Cat# A11036; RRID:AB_10563566
Alexa Fluor 633 goat anti-mouse	Life Technologies	Cat# A21052; RRID:AB_2535719
Chemicals, peptides, and recombinant proteins		
Quinine hydrochloride dihydrate	Sigma-Aldrich	Q1125
Denatonium benzoate	Sigma-Aldrich	D5765
Lobeline hydrochloride	Sigma-Aldrich	141879
Caffeine	Sigma-Aldrich	C0750
L-canavanine	Sigma-Aldrich	C1625
Sucrose	Sigma-Aldrich	S9378
All trans-retinal	Sigma-Aldrich	R2500
3-octanol (OCT)	Sigma-Aldrich	218405
4-methylcyclohexanol (MCH)	Fluka	66360
Experimental models: Organisms/strains		
<i>Drosophila</i> , Gr33a-Gal4	Moon et al. ⁴³	BDSC 31425
<i>Drosophila</i> , Gr66a-Gal4	Scott et al. ⁶⁸	Flybase: FBtp0014661
<i>Drosophila</i> , Gr98d-Gal4	Weiss et al. ³²	BDSC 57692
<i>Drosophila</i> , Gr22f-Gal4	Weiss et al. ³²	BDSC 57610
<i>Drosophila</i> , Gr59c-Gal4	Weiss et al. ³²	BDSC 57650
<i>Drosophila</i> , Gr47a-Gal4	Weiss et al. ³²	BDSC 57638
<i>Drosophila</i> , Gr64f-Gal4	Dahanukar et al. ⁶⁹	BDSC 57669
<i>Drosophila</i> , ppk28-Gal4 ⁷⁻¹	Cameron et al. ³¹	Flybase: FBtp0054514
<i>Drosophila</i> , nsyb-Gal4 ²⁻¹	Jonson et al. ⁷⁰	N/A
<i>Drosophila</i> , TH-Gal4	Friggi-Grelin et al. ⁷¹	BDSC 8848
<i>Drosophila</i> , MB320C-splitGal4	Aso and Rubin ⁵⁷	BDSC 68253
<i>Drosophila</i> , R58E02-Gal4	Liu et al. ⁷²	BDSC 41347
<i>Drosophila</i> , MB077C-splitGal4	Aso et al. ⁴⁸	BDSC 68284
<i>Drosophila</i> , MB099C-splitGal4	Aso and Rubin ⁵⁷	BDSC 68290
<i>Drosophila</i> , Gr66a-lexA	Thistle et al. ²⁹	Flybase: FBtp0125828
<i>Drosophila</i> , 25D01-lexA	Pfeiffer et al. ⁷³	BDSC 53519
<i>Drosophila</i> , UAS-GCaMP6f ^{p40}	Chen et al. ⁷⁴	BDSC 42747
<i>Drosophila</i> , UAS-NLS-RedStinger	Barolo et al. ⁷⁵	Flybase: FBtp0018199
<i>Drosophila</i> , UAS-Shi ^{ts}	Kitamoto ³⁸	Flybase: FBtp0013545
<i>Drosophila</i> , UAS-Chrimson-TdT ^{VK5}	Duistermars et al. ⁷⁶	N/A
<i>Drosophila</i> , UAS-TdT ^{VK5}	D. Hattori	N/A
<i>Drosophila</i> , lexAop-GCaMP6f ^{p5}	Hattori et al. ⁷⁷	BDSC 44277
<i>Drosophila</i> , Gr33a ¹	Moon et al. ⁴³	BDSC 31427
<i>Drosophila</i> , Gr66a ^{ex83}	Moon et al. ⁷⁸	BDSC 25027
<i>Drosophila</i> , Gr93a ³	Lee et al. ⁴⁰	BDSC 27592
<i>Drosophila</i> , UAS-Gr33a	Dweck and Carlson ⁴²	Flybase: FBtp0141160
<i>Drosophila</i> , UAS-Gr66a	Moon et al. ⁷⁸	BDSC 24775

(Continued on next page)

Continued

REAGENT or RESOURCE	SOURCE	IDENTIFIER
<i>Drosophila</i> , UAS-Gr93a	Dweck and Carlson ⁴²	Flybase: FBtp0141159
<i>Drosophila</i> , UAS-Gr39a.a	Dweck and Carlson ⁴²	Flybase: FBtp0141161
<i>Drosophila</i> , hsFLP.PEST.Opt ^{attP3}	Nern et al. ⁷⁹	BDSC 77140
<i>Drosophila</i> , FRT-Gal80-FRT	Gordon and Scott ⁸⁰	BDSC 38881
Software and algorithms		
MATLAB	Mathworks	https://www.mathworks.com
Python 3.7	Python	https://www.python.org
GraphPad Prism	GraphPad Software	https://www.graphpad.com:443/scientific-software/prism
Fiji	NIH	http://fiji.sc
Code for receptor modeling	this study	https://github.com/avdevineni/receptor-model
Code for calcium imaging analysis	Hattori et al. ⁷⁷ and Devineni et al. ⁸¹	N/A
Other		
Solenoid pinch valves for tastant delivery	Cole Parmer	EW-98302-00
Data acquisition (DAQ) device for taste delivery	Measurement Computing	USB-1408FS
Veho USB digital microscope camera	Veho	VMS-004
617 nm LED	Luxeon Star	SR-05-H2070
filters for odor delivery	Whatman	6888-2527

RESOURCE AVAILABILITY**Lead contact**

Further information and requests for resources and reagents should be directed to and will be fulfilled by the lead contact, Anita Devineni (anita.devineni@emory.edu).

Materials availability

This study did not generate new unique reagents.

Data and code availability

- All data reported in this paper will be shared upon request to the lead contact.
- Imaging analysis was performed using existing code; references are cited in the [key resources table](#) and [STAR Methods](#). Original code for computational modeling of receptor function is publicly available on GitHub; link is provided in the [key resources table](#).
- Any additional information required to reanalyze the data reported in this paper is available from the lead contact upon request.

EXPERIMENTAL MODEL AND SUBJECT DETAILS**Fly strains and maintenance**

Flies were reared at 25°C and 70% relative humidity on standard cornmeal food. Experiments were performed on 1-2 week-old flies. All flies tested were females unless otherwise specified. Flies used for optogenetic experiments were maintained in constant darkness and fed on food containing 1 mM all trans-retinal for 3-5 days prior to testing. For starvation experiments, flies were food-deprived with water (using a wet piece of Kimwipe) for the specified amount of time before testing.

Genotypes used for each experiment are specified below, and source information for fly strains is provided in the [key resources table](#).

Fly genotypes for each experiment**Figure 1**

- *Gr98d-Gal4/UAS-GCaMP6f⁴⁰* (bitter-sensing neurons)
- *Gr64f-Gal4/UAS-GCaMP6f⁴⁰* (sugar-sensing neurons)
- *ppk28-Gal4^{7.1}/UAS-GCaMP6f⁴⁰* (osmolarity-sensing neurons)

Figure 2

- *Gr98d-Gal4/UAS-GCaMP6f^{P40}* (S-a bitter neurons)
- *Gr22f-Gal4/UAS-GCaMP6f^{P40}* (S-b bitter neurons)
- *UAS-GCaMP6f^{P40}/+; Gr59c-Gal4/+* (I-a and S-a bitter neurons)
- *Gr47a-Gal4/UAS-GCaMP6f^{P40}* (I-b bitter neurons)
- *Gr33a-Gal4/UAS-GCaMP6f^{P40}* (all labellar bitter neurons)
- *hsFLP/+; Gr98d-Gal4, UAS-GCaMP6f^{P40}/+; FRT-Gal80-FRT/UAS-NLS-RedStinger* (S-a single cells)
- *hsFLP/+; Gr22f-Gal4, UAS-GCaMP6f^{P40}/+; FRT-Gal80-FRT/UAS-NLS-RedStinger* (S-b single cells)

Figure 3

- *Gr33a-Gal4/UAS-GCaMP6f^{P40}* (bitter-sensing neurons)
- *Gr64f-Gal4/UAS-GCaMP6f^{P40}* (sugar-sensing neurons)

Figure 4

- *Gr98d-Gal4/UAS-GCaMP6f^{P40}* (nerve imaging)
- *Gr33a-Gal4, UAS-GCaMP6f^{P40}/+; UAS-Shi^{ts}/+* (silencing bitter output, experimental flies)
- *Gr33a-Gal4, UAS-GCaMP6f^{P40}/+* (silencing bitter output, control flies)
- *Gr66a-lexA/lexAop-GCaMP6f; nsyb-Gal4²⁻¹/UAS-Shi^{ts}* (silencing all neuronal output, experimental flies)
- *Gr66a-lexA/lexAop-GCaMP6f; nsyb-Gal4²⁻¹/+* (silencing all neuronal output, control flies)

Figure 5

- *Gr98d-Gal4/UAS-GCaMP6f^{P40}; UAS-Chrimson-TdT^{VK5}/+* (optogenetic activation, experimental flies)
- *Gr98d-Gal4/UAS-GCaMP6f^{P40}* (optogenetic activation, control flies)
- *Gr33a-Gal4/Gr33a¹, UAS-GCaMP6f^{P40}* (Gr33a mutant; note that the *Gal4* insertion is also a *Gr33a* mutation)
- *Gr33a-Gal4/UAS-GCaMP6f^{P40}* (Gr33a heterozygous control; note that the *Gal4* insertion is also a *Gr33a* mutation)
- *Gr66a-Gal4/UAS-GCaMP6f^{P40}; Gr66a^{ex83}* (Gr66a mutant)
- *Gr66a-Gal4/UAS-GCaMP6f^{P40}; Gr66a^{ex83}/+* (Gr66a heterozygous control)
- *Gr66a-Gal4/UAS-GCaMP6f^{P40}; Gr93a³* (Gr93a mutant)
- *Gr66a-Gal4/UAS-GCaMP6f^{P40}; Gr93a³/+* (Gr93a heterozygous control)
- *Gr64f-Gal4, UAS-GCaMP6f^{P40}/UAS-Gr33a, UAS-Gr66a; UAS-Gr39a.a/UAS-Gr93a* (caffeine receptor misexpression)
- *Gr64f-Gal4, UAS-GCaMP6f^{P40}/+* (control for caffeine receptor misexpression)

Figure 6

- *UAS-GCaMP6f^{P40}/+; TH-Gal4/+* (PPL1 DANs)

Figure 7

- *UAS-GCaMP6f^{P40}/+; MB077C-splitGal4/+* (imaging $\gamma 2\alpha'1$ MBON for odor-bitter pairing experiments)
- *25D01-lexA/lexAop-GCaMP6f^{P5}; MB099C-splitGal4/UAS-Chrimson-TdT^{VK5}* (imaging $\gamma 2\alpha'1$ MBON for optogenetic pairing experiments, experimental flies)
- *25D01-lexA/lexAop-GCaMP6f^{P5}; MB099C-splitGal4/UAS-TdT^{VK5}* (line for co-staining *MB099C* and *25D01-lexA* expression)

Figure S1

- *Gr33a-Gal4/UAS-GCaMP6f^{P40}*

Figure S2

- *Gr33a-Gal4/UAS-GCaMP6f^{P40}* (male versus female flies)
- *Gr66a-Gal4/UAS-GCaMP6f^{P40}* (fed versus starved flies)
- *Gr98d-Gal4/UAS-GCaMP6f^{P40}* (testing bitter-sugar mixtures)

Figure S4

- *UAS-GCaMP6f^{P40}/+; MB320C-splitGal4/+* ($\gamma 1$ DAN)
- *UAS-GCaMP6f^{P40}/+; TH-Gal4/+* ($\alpha 2 \alpha'2$ and $\gamma 2\alpha'1$ DANs)
- *UAS-GCaMP6f^{P40}/+; R58E02-Gal4/+* (PAM $\gamma 4$ DAN)

Figure S5

- *UAS-GCaMP6f^{p40}/+; MB077C-splitGal4/+* (imaging $\gamma 2\alpha'1$ MBON in Figures S5A–S5D)
- *UAS-GCaMP6f/+; MB099C-splitGal4/UAS-Chrimson-TdT^{VK5}* (validation of DAN optogenetic activation, “+ Chrim”)
- *UAS-GCaMP6f/+; MB099C-splitGal4/UAS-TdT^{VK5}* (control for validation of DAN optogenetic activation, “- Chrim”)
- *25D01-lexA/lexAop-GCaMP6f^{b5}; MB099C-splitGal4/+* (imaging $\gamma 2\alpha'1$ MBON for optogenetic pairing experiments, control flies lacking Chrimson shown in Figure S5F)

METHOD DETAILS**Taste stimulation and calcium imaging**

Tastants were delivered to the labellum or foreleg as previously described⁸¹ using a custom-built solenoid pinch valve system controlled by MATLAB software via a data acquisition device (Measurement Computing). Solenoid pinch valves (Cole Parmer) were opened briefly (~10 ms) to create a small liquid drop at the end of a 5 μ L glass capillary, positioned such that the drop would make contact with the labellum or leg. Tastants were removed after a fixed duration by a vacuum line controlled by a solenoid pinch valve. Proper taste delivery was monitored using a side-mounted camera (Veho VMS-004), which allowed for visualization of the fly and tastant capillary using the light from the imaging laser. 5 s taste stimuli were used for all experiments unless otherwise specified. At least three trials of each stimulus were given. Other than experiments explicitly testing repeated taste stimulation, at least one minute rest was given between trials to avoid habituation. Taste stimulus durations and IPIs reported in this study refer to the values programmed in MATLAB; actual values were slightly longer and were determined by recording time stamps for valve opening and closing.

Tastants were obtained from Sigma-Aldrich (see [key resources table](#)). Unless otherwise specified, the following concentrations of tastants were used: 10 mM quinine; 10 mM denatonium; 1 mM lobeline; 10 mM (Figures 2A–2D), 50 mM (Figures 5E–5H), or 100 mM (Figures 2E, 2F, 2I, 3B, 5I, 5J, 6D, and S2E) caffeine; 25 mM L-canavanine; and 100 mM (Figures 3C, 3D, 5I, 5J, S2G, and S4D–S4F) or 500 mM (Figure 1) sucrose. L-canavanine was also tested at 50 mM and 100 mM and no OFF response was observed (data not shown), similar to the response at 25 mM. To test the effect of varying concentration (Figures 2G and 2H) we used the following concentrations: quinine at 0.1 mM, 1 mM, 5 mM, 10 mM, and 100 mM; denatonium at 0.1 mM, 1 mM, 5 mM, and 10 mM; and caffeine at 10 mM, 50 mM, and 100 mM.

Flies were imaged using previously described protocols.⁸¹ Flies were first taped on their backs to a piece of clear tape in an imaging chamber. For labellar taste stimulation, fine strands of tape were used to restrain the legs, secure the head, and immobilize the proboscis in an extended position. For leg taste stimulation, the two forelegs were immobilized using tape and parafilm with the distal segment exposed. To image sensory neuron projections in the SEZ, an imaging window was cut on the anterior surface of the head, the antennae were removed, and the esophagus was cut in order to visualize the SEZ clearly. The labial nerve was imaged ~150–200 μ m upstream of the axon terminals through a larger window. Initial experiments imaging the PPL1 DANs used a similar preparation as for SEZ imaging, but we later modified this preparation by moving the imaging window more dorsally to exclude the antennae and leave them intact. All MBON imaging experiments used the new preparation. We generally imaged the dendritic arbors of the $\gamma 2\alpha'1$ MBON within the mushroom body lobe. However, for optogenetic experiments in which the DAN was activated, we imaged the dendritic shaft of the $\gamma 2\alpha'1$ MBON just adjacent to the lobe because otherwise the DAN’s expression of *UAS-Chrimson-TdT* bled through into the GCaMP imaging channel. Imaging experiments were performed in modified artificial hemolymph in which 15 mM ribose is substituted for sucrose and trehalose.^{60,82}

Calcium imaging experiments were performed using a two-photon laser scanning microscope (Ultima, Bruker) equipped with an ultra-fast Ti:S laser (Chameleon Vision, Coherent) that is modulated by pockel cells (Conoptics). The excitation wavelength was 925 nm. Emitted photons were collected with a GaAsP photodiode detector (Hamamatsu) through a 60X water-immersion objective (Olympus). Images were acquired using the microscope software (PrairieView, Bruker). A single plane through the widest and/or brightest area of axonal or dendritic projections was chosen for imaging. For most experiments in which sensory neurons or DANs were imaged without repeated taste stimulation, images were acquired at 256 by 256 pixels with a scanning rate of 3–4 Hz. The resolution was decreased and scanning rate was increased for MBON imaging and experiments using repeated taste stimulation: ~6–7 Hz for most experiments and ~15 Hz for very short repeated taste stimulation (Figure 3D).

Single cell labeling

It is not possible to distinguish the responses of individual labellar bitter neurons when imaging axonal projections. We therefore labeled single bitter neurons by using FLP-mediated excision of the Gal4 repressor *Gal80* to sparsen bitter Gal4 expression patterns. We used a heat shock-inducible FLP recombinase that induces low levels of recombination in the absence of heat shock. In a small, random subset of Gal4-expressing neurons, *Gal80* is excised and allows Gal4 to drive expression of *UAS-GCaMP* as well as the nuclear red marker *UAS-NLS-RedStinger*. We screened hundreds of intact flies to identify those that contained exactly one labeled labellar neuron based on expression of RedStinger in the labellum, and we then imaged its axonal projections.

Shibire silencing

Imaging experiments involving *Shi^{ts}* silencing were performed similarly to previously described protocols.⁷⁷ The imaging chamber was held in a temperature-controlled platform (Warner Instruments) mounted on the microscope stage. Flies were prepared and initially imaged at room temperature (~21°). The saline was then exchanged with pre-heated saline at 32°. The temperature was constantly monitored using a small thermistor placed in the saline immediately next to the microscope objective and was maintained close to 32° by the heating system. After imaging at 32°, flies were returned to room temperature by turning off the heating system and exchanging the warm saline for room temperature saline. Post-heating responses at room temperature were similar to those recorded before heating (data not shown).

Optogenetic stimulation

Optogenetic stimulation during calcium imaging was delivered as previously described.⁷⁷ Red light was delivered using a 617 nm LED (Luxeon Star) with an attached lens. Light onset and offset were triggered using the imaging software's voltage output function through an LED controller (BuckPuck 700 mA, Luxeon Star). A high-speed shutter was closed during light delivery to protect the GaAsP detector, so images were only acquired on frames when the light was off and light delivery was timed to coincide with specific frames. For optogenetic activation and imaging of bitter sensory neurons (Figure 5B), light was turned on for every third frame: 269 ms light on, 597 ms light off, repeated 5 or 10 times for a total stimulus duration of ~4 s or ~8 s, respectively. Calcium responses were linearly interpolated during these light stimulation periods. For optogenetic activation of DANs (Figures 7H, S5E, and S5F), each light stimulus comprised a 50 ms pulse repeated 16 times with an interpulse interval of 100 ms, for a total duration of 2.3 s.

Odor-bitter pairing

Odor-bitter pairing was repeated 8 times with a 10 s inter-odor interval. A 3 s odor stimulus (the conditioned odor, CS+) was turned on 0.5 s prior to either the onset ("bitter onset pairing") or offset ("bitter offset pairing") of a 5 s bitter stimulus. In each CS+ block the odor was presented 3 times alone ("pre-pairing"), then paired 8 times with bitter ("pairing"), then again presented 3 times alone ("post-pairing"). The inter-odor interval was 10 s. CS- blocks were presented in the same way but without bitter delivery. The vacuum that removes the bitter stimulus was still presented at the same time during CS- blocks. The CS+ and CS- blocks were repeated 3 times in each fly with an interval of several minutes between blocks. The odors used were 3-octanol (OCT) and 4-methylcyclohexanol (MCH). Which odor was used as the CS+ or CS- was counterbalanced across flies. The order of CS+ and CS- blocks was also counterbalanced, i.e., half the flies experienced the CS+ block first and the other experienced the CS- block first.

Odors were delivered as previously described⁷⁷ using a computer-controlled olfactometer (Island Motion). Odors were diluted in mineral oil at 1:250 for MCH and 1:333 for OCT. 500 µL of each odor solution was pipetted onto a Whatman syringe filter and inserted into an odor mixing manifold. An odorized air stream was created by flowing air at 500 mL/min through the manifold, with valves controlling which odor filter received the air stream. This odorized air stream was mixed with a carrier air stream that had a flow rate of 1000 mL/min. The diluted odor stream (1500 mL/min) was then split equally into two streams (750 mL/min each), one directed to the fly and the other directed to a photoionization detector (mini-PID, Aurora Scientific) to monitor odor delivery. PID signals were collected using the imaging software at 50 Hz. Air flow was turned on at least one minute prior to the start of imaging experiments. Odor delivery was controlled and synchronized with bitter delivery using MATLAB.

Immunohistochemistry

Brains were dissected in phosphate buffered saline (PBS) and fixed for 15–20 min in 4% paraformaldehyde in PBS. Brains were then washed multiple times with PBS containing 0.3% Triton X-100 (PBST), blocked with 5% normal goat serum diluted in PBS for 1 hr, incubated with primary antibodies at 4° for 2–3 days, washed in PBST, incubated with secondary antibodies at 4° overnight, then washed in PBST and PBS and mounted in Vectashield. Primary antibodies used were chicken anti-GFP (1:1000), rabbit anti-DsRed (1:500), and mouse nc82 (1:10). Secondary antibodies used were Alexa Fluor 488 goat anti-chicken (1:500), Alexa Fluor 568 goat anti-rabbit (1:500), and Alexa Fluor 633 goat anti-mouse (1:500). Images were acquired on a Zeiss LSM 710 system using a 25x or 40x objective. Confocal images were processed using Fiji/ImageJ.

Computational modeling of receptor function

Computational modeling of receptor function was implemented in MATLAB (code available here: <https://github.com/avdevineni/receptor-model>). A deterministic model was used to model a population of receptors. Receptor states are described by the variables m , representing receptor opening ($m = 1$ represents an open receptor), and h , representing receptor inactivation ($h = 0$ represents an inactivated receptor). Individual receptors can be in one of four states: open and active ($m = 1, h = 1$), open and inactive ($m = 1, h = 0$), closed and active ($m = 0, h = 1$), or closed and inactive ($m = 0, h = 0$). Because we are modeling a receptor population, m and h can take on any value between 0 and 1, which represents the fraction of receptors in the corresponding state. Only receptors in the open and active state can pass current, so receptor current at each time is quantified as $m \cdot h$. This is also referred to as "receptor output" or "normalized activity." Receptors transition between states based on rate constants that are free parameters in the model. The rates were allowed to vary depending on whether the receptor was bound to the ligand, but we set the rates to be the same whenever possible. Bitter presentation shifted all receptors into the bound state at the specified time. For the main model, the following rates were used:

$R_{closed > open, unbound}$ (closed to open, when unbound): 0
 $R_{closed > open, bound}$ (closed to open, when bound): 20
 $R_{open > closed}$ (open to closed, when bound or unbound): 0.5
 $R_{active > inactive, unbound}$ (active to inactive, when unbound): 0.1
 $R_{active > inactive, bound}$ (active to inactive, when bound): 0.4
 $R_{inactive > active, unbound}$ (inactive to active, when unbound): 100
 $R_{inactive > active, bound}$ (inactive to active, when bound): 0

We used timesteps of 0.001 for the figures shown in the paper; timesteps of 0.0001 also yielded the same results. At each time t , m and h are calculated based on the following equations:

$$m(t) = m(t-1) - R_{open > closed} * dt * m(t-1) + R_{closed > open} * dt * (1 - m(t-1))$$

$$h(t) = h(t-1) - R_{active > inactive} * dt * h(t-1) + R_{inactive > active} * dt * (1 - h(t-1))$$

For $m(t)$, this represents starting with $m(t-1)$, subtracting the fraction of open receptors that closed, and adding the fraction of closed receptors that opened. Similarly for $h(t)$, this represents starting with $h(t-1)$, subtracting the fraction of active receptors that inactivated, and adding the fraction of inactive receptors that de-inactivated. The appropriate rate is chosen depending on whether the receptor is bound.

After exploring the parameter space, parameters were chosen to generate realistic ON and OFF responses. We set the opening rate when unbound ($R_{closed > open, unbound}$) to zero for simplicity, but a non-zero rate yields similar results as long as the rate is substantially higher in the bound state ($R_{closed > open, bound}$). The opening rate when bound ($R_{closed > open, bound}$) determines the ON response rise time. In the model the decay of the ON response is mediated by receptor inactivation, whereas the decay of the OFF response reflects receptor closing. The closing rate ($R_{open > closed}$) was set to a low value in order to generate an OFF response that persists for several seconds. For simplicity, we set the closing rate to be the same regardless of whether the receptor is bound. The de-inactivation rate (inactive to active) was set to zero when the receptor is bound, meaning that inactive receptors do not de-inactivate until bitter is removed. The rapid de-inactivation upon bitter removal generates the OFF response. We note that the model simulates receptor current, whereas the experimental data represent GCaMP responses. Thus our estimation of the rate constants in the model are likely affected by the slower kinetics of calcium and GCaMP signaling.

Four parameters were varied to mimic the dynamics elicited by different ligands:

- 1) Closing rate ($R_{open > closed}$): 0.5 for quinine, 0.3 for denatonium, 0.65 for lobeline, 2.0 for L-canavanine.
- 2) Inactivation rate when bound ($R_{active > inactive, bound}$): 0.3 for quinine and denatonium; 0.15 for lobeline and L-canavanine.
- 3) Inactivation rate when unbound ($R_{active > inactive, unbound}$): 0.1 for quinine, denatonium, and lobeline; 0.01 for L-canavanine.
- 4) De-inactivation rate when unbound ($R_{inactive > active, unbound}$): 100 for quinine, denatonium, and lobeline; 0.5 for L-canavanine.

Habituation was implemented as a factor H that modulates receptor current, such that current is now quantified as m^*h^*H . H implements a suppression of receptor output based on the number of previous stimuli, modeled by an exponential decay function. This approach is agnostic as to whether graded habituation reflects a graded decrease in the output of individual receptors or an all-or-nothing suppression of receptor output that occurs in varying fractions of the receptor population. H varies depending on whether the receptors are bound; this was implemented by using different tau values for the exponential decay curves (1.8 for the bound state and 15 for the unbound state).

QUANTIFICATION AND STATISTICAL ANALYSIS

Calcium imaging analysis

Calcium imaging data were analyzed using MATLAB code from previous studies.^{81,77} In most experiments, images were registered within and across trials to correct for movement in the x-y plane using a sub-pixel registration algorithm. Regions of interest (ROIs) were drawn manually. Average pixel intensity within the ROI was calculated for each frame. The average signal for 20 frames preceding stimulus delivery was used as the baseline signal, and the $\Delta F/F$ (change in fluorescence divided by baseline) for each frame was then calculated. The peak ON response was quantified as the average $\Delta F/F$ value for the two highest consecutive frames during stimulus presentation. The peak OFF response was quantified in the same way for the 2.5 s following stimulus offset, except that the $\Delta F/F$ value just prior to stimulus removal (average over last two frames) was then subtracted. The OFF response therefore represents how much the calcium activity increases upon stimulus offset. We believe that this is a more appropriate method than comparing OFF activity to the pre-stimulus baseline, which would make the OFF response highly dependent on the value of the ON response at the end of the stimulus presentation. ON response adaptation was quantified as $1 - (\text{average response on last two stimulus frames} / \text{peak ON response})$. Trials were excluded if the tastant drop failed to make proper contact with the leg or labellum based on video monitoring. In some leg stimulation experiments (Figures 1C and S1A) responses were not evoked on every trial and non-responsive trials were excluded from the averages.

For MBON imaging experiments the plasticity effect was calculated as follows: we separately averaged the CS+ and CS- responses across all blocks, then calculated the percent change from pre-pairing to post-pairing, and finally calculated the difference

between these values for the CS+ and CS-. Because this method generates a single value for each experiment, we performed bootstrapping in MATLAB using 10000 iterations to obtain an estimate of the standard deviation. When quantifying odor responses during bitter offset pairing in [Figure 7E](#), we only averaged the initial odor response before the vacuum turned on because the vacuum induced a change in airflow that led to MBON activation (see [Figure S5D](#)). However, the entire odor response was averaged to calculate the plasticity effect ([Figure 7F](#)), since this analysis does not require consideration of paired trials.

Statistical testing

To determine whether the plasticity effect of each MBON imaging experiment was statistically significant (compared to zero), we performed permutation testing in MATLAB using 10000 permutations. All other statistical analyses were performed using GraphPad Prism, Version 4. Statistical tests and results are reported in the figure legends. To compare two groups, a t test was used when sample sizes were similar and the non-parametric Mann-Whitney test was used when sample sizes were disparate. One- or two-way ANOVA was used to compare multiple groups with Tukey's or Bonferroni's post-tests, respectively. All graphs represent mean ± SEM unless otherwise specified. Sample sizes are listed in the figure legends and the number of trials and flies is noted.

Decoding analysis

For decoding analyses, GCaMP traces were first normalized to the maximum response of each fly. ON and OFF responses were each quantified by multiple “features” representing the average response over different time windows. We compared decoding results using different numbers of features and found that just two features per response enabled decoding with similar accuracy as 4 or 8 features. These two features represented the “early” response (first 3 frames or ~0.8 s) and the “late” response (last two frames or ~0.6 s). Each feature was then scaled to the same range. Decoding analyses were performed using support vector classification with a linear kernel using the scikit-learn library in Python. Decoder performance was quantified using k-fold stratified cross-validation, which was iterated 1000 times to ensure data were randomly allocated into “folds” (i.e., training and testing sets), and the average accuracy across iterations was calculated. For decoding with shuffled labels, the same cross-validation analysis was performed for 100 random shuffles of the labels, except that allocation of data into each fold was only iterated 10 times per label shuffle (representing 1000 total iterations), and the average accuracy was calculated.